

AD-A068 491

SOLAR TURBINES INTERNATIONAL SAN DIEGO CA
EFFECTS OF GAS TURBINE COMBUSTION ON SOOT DEPOSITION. (U)

F/6 21/2

UNCLASSIFIED

MAR 79 D J WHITE
SR79-R-4643-03

N00014-78-C-0003

NL

| OF |
AD
A068491



END
DATE
FILED
6-79
DDC

LEVEL II

12

ADA068491

Effects of Gas Turbine Combustion on Soot Deposition

FINAL REPORT

Contract No. N00014-78-C-0003

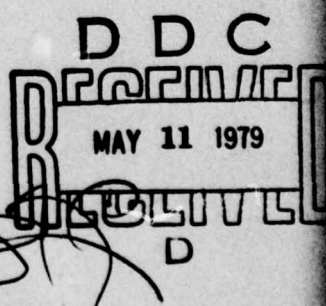
541,693 (2)

DDC FILE COPY

Approved for public release; distribution unlimited.

Reproduction in whole or part is permitted for any
purpose of the United States government.

This research was sponsored by the Office of Naval
Research under contract No. N00014-78-C-0003



SOLAR TURBINES INTERNATIONAL
An Operating Group of International Harvester
2200 Pacific Highway, P.O. Box 60966, San Diego, California 92136

79 05 10 003

12
LEVEL

SR79-R-4643-03

11 March 1979

14 SR79-R-4643-03
6-4643-7

6

Effects of Gas Turbine Combustion on Soot Deposition .

FINAL REPORT

Contract No. N00014-78-C-0003

15

12) 59P

by

10 D.J. White

9

Final rept. 15 Oct 77-Mar 79,

for

Office of Naval Research
Department of the Navy
800 N. Quince Street
Arlington, Va 22217

Approved for public release; distribution unlimited.

Reproduction in whole or part is permitted for any
purpose of the United States government.

This research was sponsored by the Office of Naval
Research under contract No. N00014-78-C-0003

AMENDMENT 14	
BY	White Carter
DDU	DDU Carter
REBOUNDED	<input checked="" type="checkbox"/>
JUSTIFICATION	<input type="checkbox"/>
BY	
DISTRIBUTION/AVAILABILITY CODES	
ON	AVAIL. AND/OR SPECIAL
A	



SOLAR TURBINES INTERNATIONAL
An Operating Group of International Harvester
2200 Pacific Highway, P.O. Box 80966, San Diego, California 92138

326 550

9m

TABLE OF CONTENTS

<u>Section</u>		<u>Page</u>
1	SUMMARY	1
2	INTRODUCTION	3
	2.1 Problem Statement	3
	2.2 Justification	3
	2.3 Initial Hypotheses	4
	2.4 Proposed Mechanism	5
3	EXPERIMENTAL PROCEDURE	7
	3.1 Test Apparatus	7
	3.2 Facility	9
	3.3 Instrumentation	12
	3.3.1 Total Hydrocarbon Measurement	13
	3.3.2 Carbon Monoxide Measurement	14
	3.3.3 Carbon Dioxide Measurement	15
	3.3.4 Oxides of Nitrogen Measurement	16
	3.4 Test Operations	19
4	RESULTS AND DISCUSSION	21
	4.1 Test Objective	21
	4.2 Test Results	22
	4.3 Discussion	34
	4.4 Deposition	34
	4.5 Particle Formation	41
	4.5.1 Nucleation	42
	4.5.2 Growth	43
	4.5.3 Agglomeration	45
	4.6 General	48
5	CONCLUSIONS AND RECOMMENDATIONS	49
	REFERENCES	51
	DISTRIBUTION LIST	53

LIST OF FIGURES

<u>Figure</u>	<u>Page</u>
1 Combustor Test Apparatus	8
2 Variable Geometry Details	8
3 General View of Combustor Showing Fuel Lines and Instrumentation	9
4 Cooled Soot Collector Tube Section	10
5 Front View of Soot Collector Tube	10
6 Rear View of Soot Collection Tube	10
7 Water Cooled Gas Sampling Probe	11
8 Smoke Sampling Probe	11
9 Soot Test Rig	12
10 Beckman Model 402 Hydrocarbon Analyzer	14
11 Beckman Model 315A Infrared Analyzer	15
12 Thermolectron Corporation Chemiluminescent Analyzer Model 10A	17
13 Von Brand Smokemeter	18
14 Possible Reaction Sequence for Soot Formation	23
15 Probable Soot Deposition Rates With Combustion System Parameters	24
16 Front View of Soot Collection Tube With Soot Coating	26
17 Soot Deposits in Combustor Exhaust	26
18 Soot Deposits in Combustor Exhaust	26
19 WFRA-RED Absorption Spectra of Soot in CS ₂	27
20 Smoke/Soot Particles on Filter Paper	29
21 Smoke/Soot Particles on Filter Paper	29
22 Single Fiber Showing Small Particles	30
23 Compound Agglomerate Soot Particle	30
24 Detail of Smoke/Soot Particle	31
25 Detail of Smoke/Soot Particle Showing Typical Botryoidal Structure	31

LIST OF FIGURES (Contd)

<u>Figure</u>		<u>Page</u>
26	Agglomerate Smoke Particle Showing Botryoidal Structure	32
27	Smoke/Soot Particle on Filter Paper	32
28	Detail of Particle of Figure 26	33
29	Detail of Particle of Figure 26	33
30	Diffusion Scheme for an Adsorbing Surface	35
31	Theoretical Inertial Collection Efficiencies for a Cylindrical Body	39
32	Experimental Inertial Collection Efficiencies for a Cylindrical Body	40
33	Deposition Rate on a 2.5 cm Tube	41

LIST OF TABLES

<u>Table</u>		<u>Page</u>
1	Test Conditions	20
2	Soot Producing Conditions	24
3	Inorganic Analysis	26
4	Approximate Size Range for Various Deposition Mechanisms	28
5	Gas-Phase Reaction Mechanism and Rate Coefficients	44
6	Particle Radii and Growth Rate Terms	46
7	Coagulation Rate Terms	47

1

SUMMARY

The original hypotheses that the program was based on were found to be wanting. Utilizing the results obtained new hypotheses have been formulated which explain not only the results of the present work but those of other investigators as well.

As originally envisioned the program was to produce a map of soot producing conditions in terms of fuel-air "premixedness" and equivalent ratio for different operating conditions. In addition the soot was to be analyzed to see whether or not the theory of soot adhesion via thermally stable polycyclic aromatic hydrocarbons (PCHH), was valid.

Using a combustion apparatus that had carefully controlled reaction or primary zone conditions, it was found that the fuel-air premixing completely dominated soot production. Even with low levels of premixing at rich conditions soot could be eliminated. Soot particles as collected on the water cooled boiler simulation tube and from the smoke sampling apparatus were found to be essentially pure carbon. Soot from the tube, however, was determined to consist of carbon with some water. Water through adsorption forces has been postulated as the "glue" that provides adhesion of carbon particles to boiler tubes. The theory of carbon condensing directly from carbon vapor in fuel rich areas has also been proposed as the mechanism for soot particle production.

2

INTRODUCTION

2.1 PROBLEM STATEMENT

Soot particle production in marine gas turbine combustors was at one time mainly an aesthetic problem associated with visible plume production, from the exhaust stack. With the advent of waste heat recovery as a means of improving overall power generation efficiencies (such as combined cycle arrangements), soot production and subsequent deposition on exhaust heat exchangers or boilers has been identified as a major operating problem.

The deposition of soot on heat exchanger surfaces is in effect a byproduct of the design. In general such heat exchangers are designed to maximize convective heat transfer within the constraints of pressure drop, cost and weight. However, when the convective heat transfer is maximized so is the convective mass transfer, and thus an effective heat exchanger is also an effective small particle collection device.

Periodic cleaning is the only method proposed for use at present to remove soot materials deposited on the hot gas side of such marine heat exchanger systems. Two such cleaning approaches are being considered. The first is the common practice of mechanical cleaning in which steam, air or water jets blow or wash the soot off surfaces. A second approach being advanced by Solar is based on the use of high surface temperatures to "burn-off" the deposits. The first of these approaches loses power during shut-down and also uses parasitic power for cleaning, while the second approach simply uses extra fuel during the cleaning process. Both approaches have many design, cost and operating penalties that indicate that a directed research effort was needed to eliminate the problem at its source.

By eliminating soot production the above processes would no longer be required and substantial cost and energy savings could be made. The work reported on herein, was concerned with determining under controlled conditions the important combustion parameters that govern soot production. With such parameters defined it was then intended to provide "maps" of soot producing conditions.

2.2 JUSTIFICATION

At present the cost of fuel and the anticipated future costs are such that it is now economically advantageous to consider heat recovery systems for both

industrial and marine gas turbine units supplying electrical or shaft-power. Of the various heat recovery approaches the one that has been chosen by Solar as the most attractive is that involving turbine exhaust heat recovery through steam generation and its subsequent use in a steam turbine to provide power. Typically the exhaust from gas turbines can produce steam at 426°C and 17 atm, together with lower pressure steam at 3.4 atm and 450°C, which would be used in a two-stage steam turbine to generate shaft-power. The attractiveness of this approach is that the technology required is largely available, and in addition it lends itself to automatic operation.

The United States Navy is presently pursuing the development of a gas turbine ship propulsion unit combined with an exhaust heat steam "bottoming cycle" which will improve the specific fuel consumption. A reduction in fuel consumption is usually reflected in reduced operating costs, increase range or increased payload.

Soot deposition on the boiler of such units is one of the major problems impeding implementation of this technology. In addition, the cleaning of soot from boilers can expose personnel (and the general public if the soot is blown into the atmosphere) to possible health hazards, because of the possibility that carcinogens could be contained in soot. The most desirable solution for any application is to eliminate the problem. Such an approach however, requires a detailed knowledge of how exhaust heat exchanger deposition is influenced by combustor operating conditions. At present this information is not available in the literature. If it were made available it would assist manufacturers of gas turbines to modify their equipment to eliminate soot production. This would eliminate down-time for cleaning which would allow vessels to have much longer operational periods.

2.3 INITIAL HYPOTHESES

The work performed was based largely on two hypotheses that were derived in part from reviews of the literature and in part from in-house work performed at Solar.

The first of the two hypotheses concerned the mechanism whereby soot particles adhered to the surface of the heat exchanger. It was postulated that certain polycyclic aromatic hydrocarbons (PCAH) which were thermally stable (and had been found by previous investigators (Ref. 1) in soot) could condense on cool surfaces and act as a "glue" to ensure the adhesion of the soot.

In the second hypothesis a model was proposed in which soot particle formation occurred in the primary zone of the combustor in high temperature fuel rich pockets. These particles were carried out of the combustor in the scheme above and were thought to separate from the gas stream and hit the heat exchanger or boiler tubes through inertial impaction.

2.4 PROPOSED MECHANISM

It was found that the material adhering to the tubes was in general pure carbon particles wetted with a film of water which was also on the tube surface. Although at present there is no definite proof, there is the above evidence that water adsorbed on the oxide layers of the Hastelloy-X tube used, and which is also in turn adsorbed onto impacted soot particles is the means by which soot adheres.

Soot particles sampled from the gas stream were measured and were found to be mostly in the range (less than 10 microns in diameter) where inertial impaction is unlikely. Generally it is believed that most of the soot particles were conveyed to the surface by turbulent diffusion. Some smaller particles of the order of 0.1 micron in diameter were probably carried to the tube surface by molecular diffusion type mechanisms.

Soot formation, it was found, was most easily eliminated by providing improved fuel-air mixing. Premixing of the air and fuel was by far the most important factor in preventing soot formation. This parameter overshadowed even the fuel-air ratio effects. This latter variable did have, however, some second order effects on soot formation prevention.

3

EXPERIMENTAL PROCEDURE

3.1 TEST APPARATUS

The test apparatus utilized was originally produced by Solar Turbines International for an evaluation of the effects of variable geometry on combustion emissions and operating range. It was an ideal vehicle, however, for an investigation of soot formation because it could provide controlled conditions within the primary or reaction zone. Controlled conditions in the sense used here refers mainly to the fact that there was essentially a single value to the fuel air ratio supplied. Most conventional gas turbine combustion systems inject fuel directly into the reaction zone thus allowing the combustion process to take place at a variety of fuel-air ratios. In the apparatus used (see Fig. 1 for a schematic) the fuel was injected into the inlet of four circular tubes or ducts. The primary or reaction air also entered through these same tubes. These tubes were sized as to length to provide a well mixed and vaporized fuel-air mixture. Thus the fuel-air charge was well dispersed or mixed before it entered the primary or reaction zone. By changing the inlet air temperature the degree of prevaporation could be increased or decreased at will. In addition mounted at the inlet to each duct was a tapered plug valve arrangement. These plugs could be moved into or out of the tube mouth to vary the air flow entering the primary or reaction zone. A similar set of plugs was also mounted to the dilution ports to control the air flow entering at this point. By controlling both the above air flows (dilution and primary) a large range of flow split ratios could be obtained without changing the overall pressure drop. Being able to maintain the pressure drop constant at some desired value while changing the flow split between primary and dilution ensures that the inlet velocity and thus the atomization quality does not change. Details of the variable geometry or valved port inlets can be seen in Figures 2 and 3. These also show the fuel injection and supply line system.

The combustor was designed and fabricated with a double wall, air was constrained to enter this annular passage and this air cooled the walls convectively. At certain points this heated cooling air was injected into the combustor as a film. As can be seen from Figure 1 there are two rows of small holes in an area that is part-way along the outer wall of the primary zone. A solid ring divided the air flow entering these two rows of holes so that the row nearest the primary zone dome (front end) fed air into a passage that lead to the dome where it was injected as a wall film for extra cooling. The air on the downstream side of the solid ring flowed rearward and eventually was injected at the combustor exit. Extra cooling is admitted to this latter passage at these points where rows of small holes are shown.

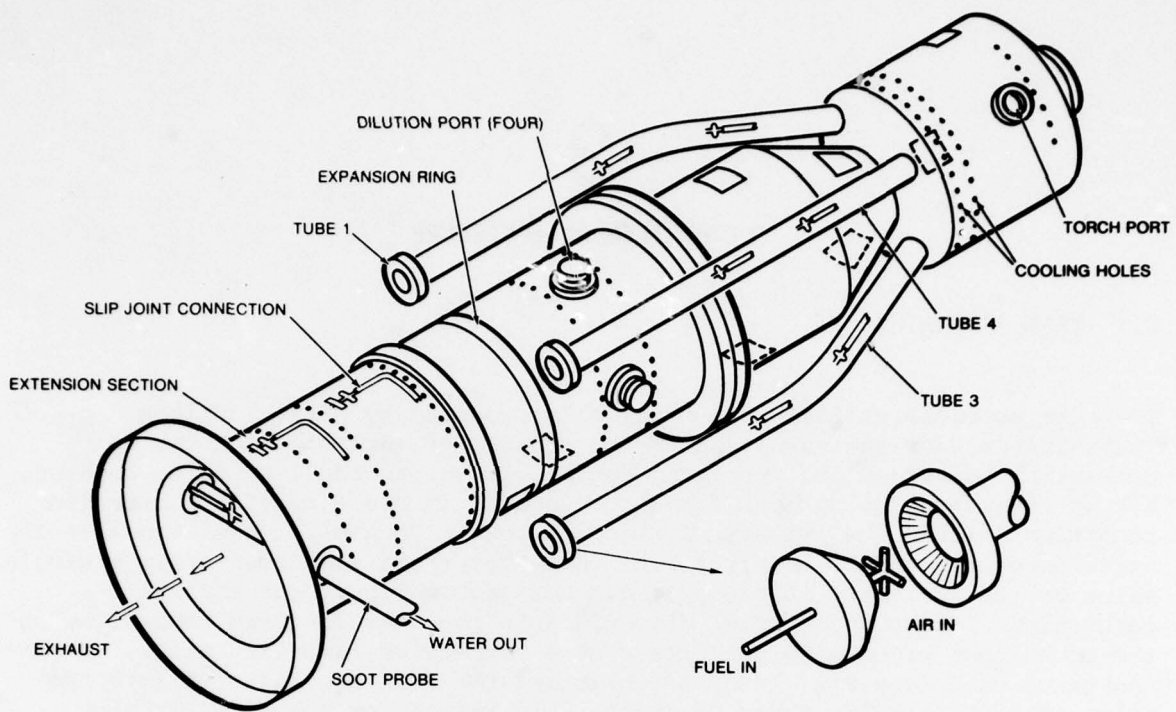


Figure 1. Combustor Test Apparatus

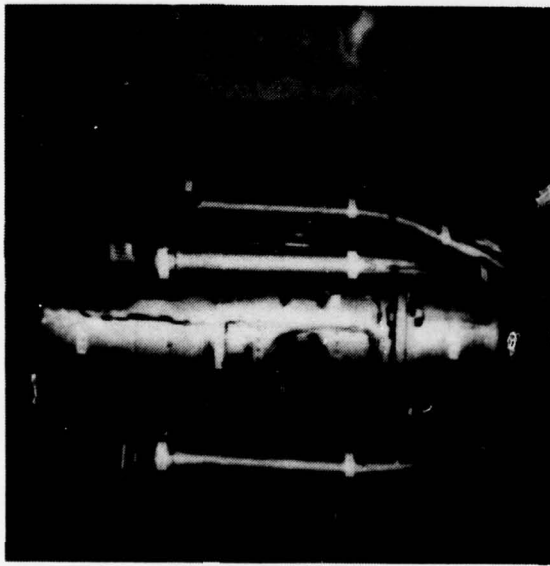


Figure 2.
Variable Geometry Details

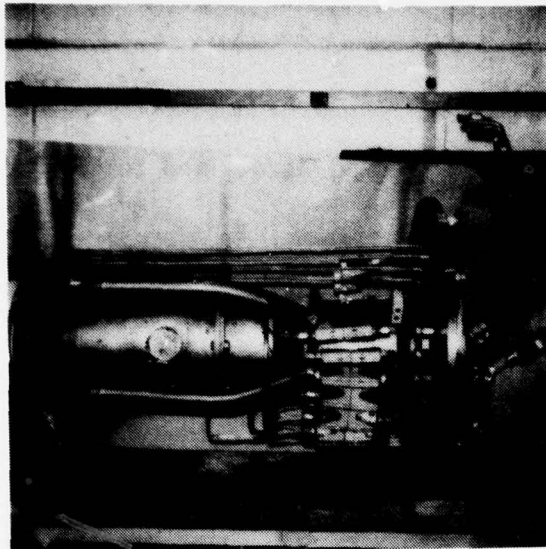


Figure 3.

General View of Combustor Showing Fuel Lines and Instrumentation

A short extra section was designed and built to fit onto the exit of the combustor proper. This section held the water cooled Hastelloy-X tube which was intended to simulate the tubes at the cold-end of a boiler. Figure 4 shows the air cooled section holding the simulated boiler tube. The boiler tube simulator itself is shown in Figures 5 and 6. These two views are front and rear respectively. A sample probe (water cooled) for obtaining emissions was located downstream of the soot collecting tube. This particular probe was of a single diametrical arrangement with seven equal area positioned sample holes or ports as shown in Figure 7. An additional probe at right angles to the above unit and located just upstream of the simulated boiler was used for smoke sampling (Fig. 8).

Once through high pressure water-cooling of the probe gas sampling was used with the water entering through one end and being ejected from the other. Downstream of this probe water (high pressure) was injected directly into the gas stream. This water both cooled the exhaust gases and the butterfly back-pressure valve which was located directly behind the sampling section.

Downstream or behind the backpressure valve was an exhaust silencer which directed the exhaust gases into a stack. This latter unit had extra cooling water injected for mechanical integrity purposes.

3.2 FACILITY

The test apparatus described above was mounted in a specially equipped test cell, that could provide air at pressures up to 12 atm, with mass flows of the order of 1.5 kg/s. this air could be preheated with an externally fired heat exchanger to provide temperatures up to 500°C (see Fig. 9). Control of the air supply was accomplished with conventional pneumatic actuated valves and regulators.



Figure 4.

Cooled Soot Collector Tube Section

Figure 5.

Front View of Soot Collector Tube

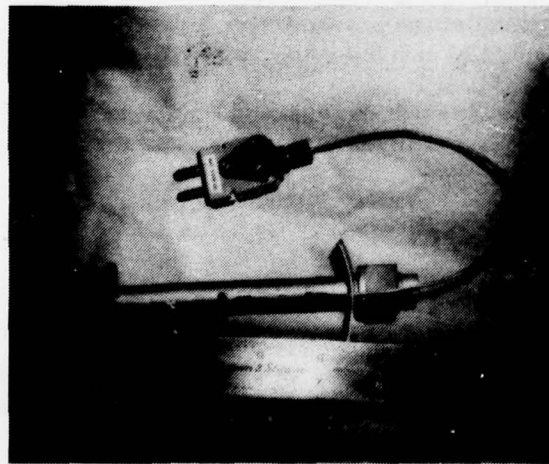
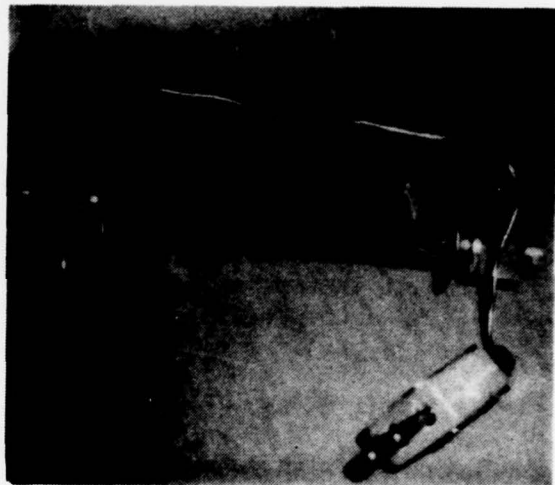


Figure 6.

Rear View of Soot Collection Tube

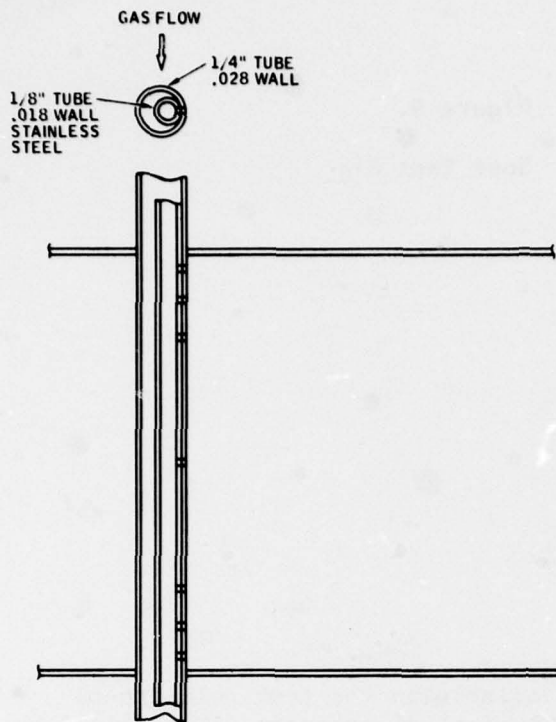


Figure 7.

Water Cooled Gas Sampling Probe

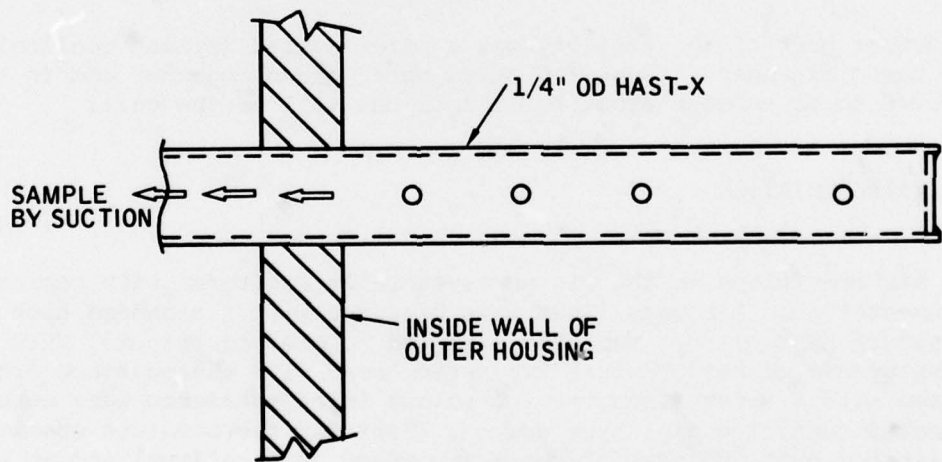


Figure 8. Smoke Sampling Probe



Figure 9.

Soot Test Rig

High pressure fuel systems were also available in the test cell; these included natural gas, DF-2 and JP-5. The fuel of interest, JP-5, could be provided at mass flow rates as high as 0.5 kg/s, at pressures between 50 and 60 atm.

Cooling water was also piped into the test cell and pressures up to 100 atm and flow rates of approximately 1 kg/s could be obtained.

Included as part of the facility was a water cooled (splash cooling) butterfly valve and a silencer. These two units were joined together and in turn were connected to an exhaust stack built into one wall of the cell.

3.3 INSTRUMENTATION

Inlet air conditions to the rig were generally monitored with conventional instrumentation. Air mass flows were measured with a standard high temperature ASME orifice run close-coupled to the rig proper. This orifice run employed a corner pressure tap arrangement with the pressure drop obtained measured with a water manometer. Absolute inlet pressures were measured with calibrated sensitive dial type gauges. Taps for the absolute static pressure were located just upstream of the sharp-edged orifice (two) and at the inlet to the rig (four). Total temperatures of the inlet air were measured upstream of the orifice and at the inlet to the rig proper. At the orifice inlet temperature plane four type K thermocouples were used and these were connected so as to read an average temperature value. A similar four thermocouple arrangement was used at the inlet to the rig. All temperatures were read from digital meters.

The other inlet parameters monitored were those associated with the fuel injection. Fuel flow rates were measured with commercial turbine meters. Pressures throughout the fuel system were all measured with accurate dial gauges. These included the pressure at the pump exit and before and after the external fluidic orifices that divided the fuel between the various combustor ports. Because of the relatively low fuel flows provided at each of the ports, flow control was not accomplished at the fuel injector orifice. If the flow were to be controlled by the injector orifice, it would require an orifice size of the order of 0.025 mm which is undesirable because of dirt blocking effects. Thus external swirl type fluidic orifices were utilized which have large actual orifices that behave as small ones and thus do not block readily. Fuel inlet temperatures (to the rig) were monitored with a single type K thermocouple, the reading from which was displayed on a digital meter.

The combustor exhaust conditions were monitored, for total temperature, static pressure, gaseous emissions, smoke and soot deposits. Eight type K thermocouples with their tips located at the center of equal area annulii were mounted in the exhaust section downstream of the soot collecting probe but upstream of the sampling probes, to monitor the exhaust temperature. The temperature indicated by each thermocouple could be read separately, or their output could be combined to provide an average value. Static pressure taps were located in a plane close by the plane where the thermocouples were located. Four static pressure taps were provided and by manifolding these together a single average output value was obtained.

The two sample probes located one behind the other and at right angles to each other were positioned at two planes. The smoke sampling probe was located at the temperature measuring area and the emissions probe a few centimeters behind it. The emission probe consisted of two tubes mounted inside one another in an eccentric manner (see Fig. 7 for construction) with cooling water passing between the two in the annulus thus formed. Exhaust gas was sampled through a series of holes in this latter probe, each of the holes being located at the center of an equal area division. It should be noted that although the probe spanned a single diameter, the section that it was mounted in could be rotated so that the emissions at different radial conditions could be determined.

The water cooled probe was designed to reduce the exhaust gas sample temperature rapidly to a temperature of approximately 150°C. After leaving the sample probe the gases were conveyed into an electrically heated Teflon sample line. This line took the sample gases from the rig to an emissions train consisting of the following.

3.3.1 Total Hydrocarbon Measurement

The total unburned hydrocarbon in the exhaust was determined continuously by the flame ionization detector method. In this method, carbon atoms were "counted" as electrical charge pulses as the sample was passed through a

hydrogen flame. The instrument was calibrated using standardized mixtures of methane in nitrogen to develop a correlation for the range of interest.

Instrument - Beckman Model 402 (Fig. 10)

Flame ionization detector, high temperature

Instrument response time 0.5 second to 90 percent

Sensitivity 0.5 percent full scale accuracy ± 1 percent

Detection range one ppm to 250,000 ppm methane

3.3.2 Carbon Monoxide Measurement

Carbon monoxide was determined by the nondispersive infrared method (NDIR). The exhaust gas sample was collected in this method as described with a water cooled stainless steel averaging probe and was partially dried by passage through a large cannister of non-indicating Drierite. Further sample processing included the removal of water by refrigeration to a constant dewpoint and filtering through a five micron filter.

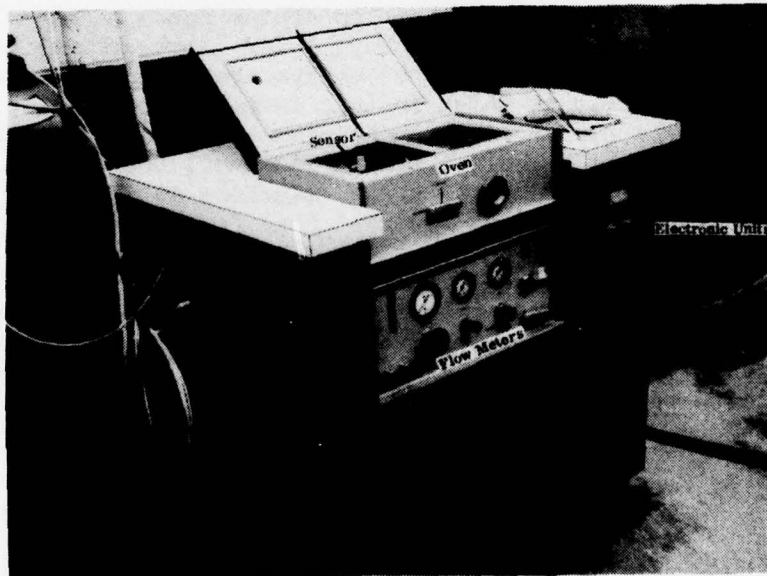


Figure 10. Beckman Model 402 Hydrocarbon Analyzer

Instrument - Beckman Model 315 Dual Stacked Cell Infrared Analyzer (Fig. 11)

Sensitivity 0.5 percent of full range
Response 0.5 seconds to 90 percent
Accuracy ± 1 percent
Range 10-inch cell 0-250 ppm, 0-1000 ppm
0.125-inch cell 0-2.5 percent

3.3.3 Carbon Dioxide Measurement

Carbon dioxide is a nontoxic combustion product and was not determined from a standpoint of pollution. It was used however as a method for checking fuel/air ratios, and in calculating carbon balances. Carbon dioxide was determined by the non-dispersive infrared method. The exhaust sample was collected with a stainless steel averaging probe and was partially conditioned by passing the sample through a cannister of non-indicating Drierite. Further sample conditioning included the removal of water by refrigeration to a constant dewpoint and filtering through a five micron filter.



Figure 11. Beckman Model 315A Infrared Analyzer

Instrument - Beckman Model 315 Infrared Analyzer (Fig. 11)

Range 0-5 percent and 0-16 percent
Response time 0.5 second to 90 percent
Sensitivity 0.5 percent of full scale
Accuracy ± 1 percent

3.3.4 Oxides of Nitrogen Measurement

The oxides of nitrogen (NO_x) were determined by the chemiluminescence method. This is a chemical method based on the reaction of nitric oxide and ozone yielding nitrogen dioxide and oxygen. In this method a fraction of the nitrogen dioxide is excited to an unstable state and decays, giving off photons. The emission is measured by a photomultiplier tube and is proportional to the nitric oxide in the system. The method also utilizes the principle that thermal decomposition of nitrogen dioxide is complete at 600°C. In this manner all the NO₂ in the sample is converted to NO before entering the reaction chamber.

The exhaust sample was drawn from the mixing chamber through a heated Teflon sample line maintained at 200°F and was transported to the instrument in this manner. The sample gas was filtered through a ten micron filter before passing into the analyzer.

Instrument - Thermo Electron Corp. Chemiluminescent Analyzer Model 10A (Fig. 12)

Equipped with a high-temperature thermo-reactor
Response time 2-4 seconds
Accuracy ± 1 percent
Sensitivity 0.1 ppm
Range 0-2 ppm full scale to 0-10,000 NO_x
Calibrations are made by the use of standard gas mixtures. The instrument is linear over all ranges. The chemiluminescent analyzer detects only nitric oxide but can be used for NO₂/NO mixtures by converting the NO₂ to NO prior to analysis.

The smoke sampling probe which was a single uncooled Hastelloy-X tube with area-weighted sample holes (see Fig. 8) conveyed the sample to a Von Brand smoke meter. This latter instrument is shown in an exploded view in Figure 13. In operation the unit compares the reflectivity of a section of filter paper that the sample has passed through with an unused portion. Changes in reflectivity indicate the presence of air borne particles. For qualitative indications of particles the filter paper which is a machine fed strip can be stopped for any desired length of time to accumulate enough particles to affect the reflectivity. This is the mode that the unit was used in for the activity described herein. It was found that a fibration dwell-time of approximately 120 seconds was sufficient to detect conditions that led to soot deposition.

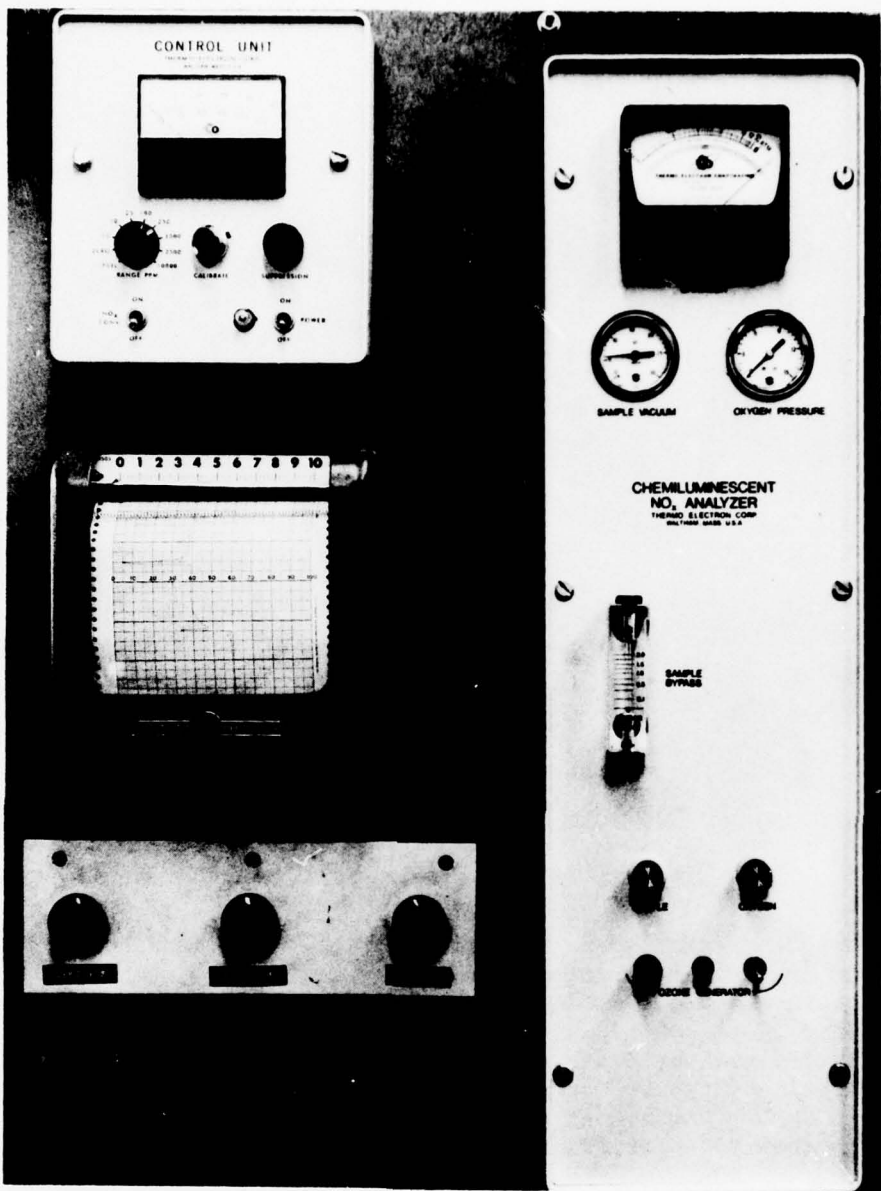


Figure 12. Thermoelectron Corporation Chemiluminescent Analyzer Model 10A

Soot was obtained from the surface of a water cooled probe which was described earlier. The soot collected mechanically from the surface of the tube was subject to a variety of analyses by several different instruments. Primarily the soot was analyzed by pyrolysis gas chromatography. In this method adsorbed, absorbed or chemically bound hydrocarbon molecules on the main carbon matrix were exposed to hot helium gas. The helium stream then conveyed

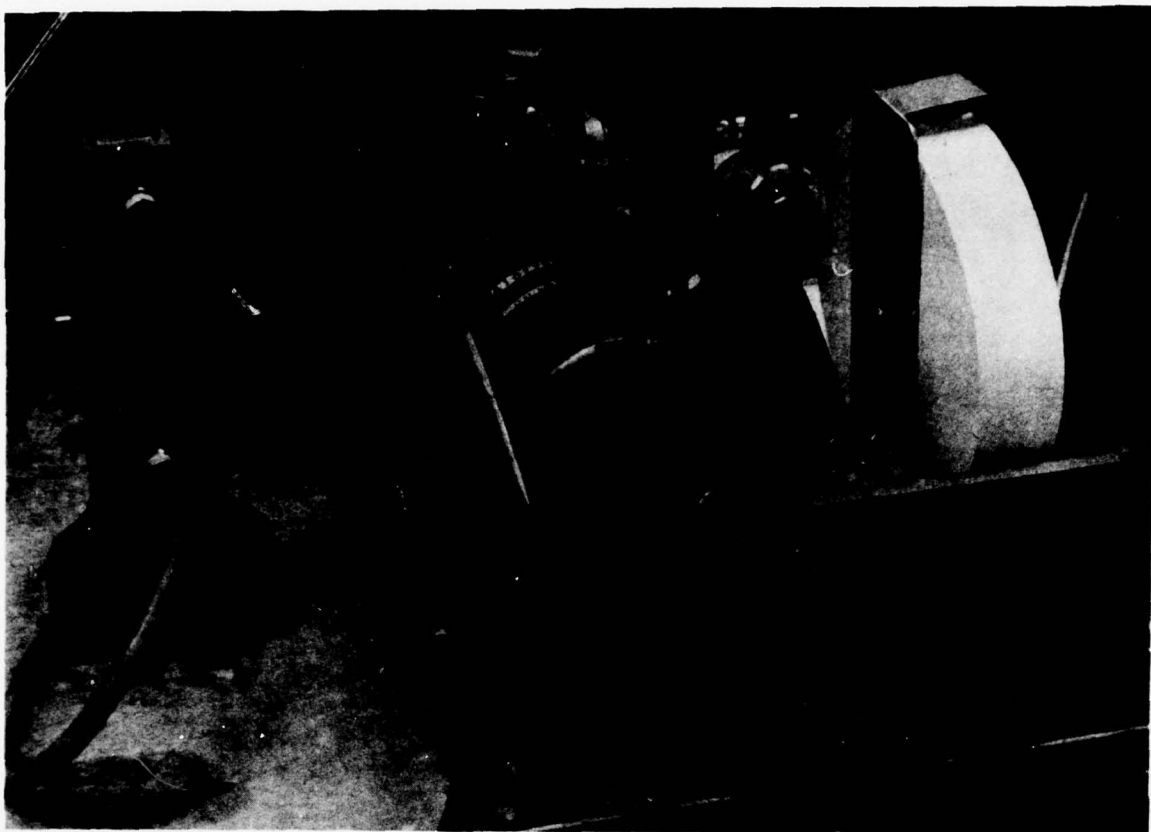


Figure 13. Von Brand Smokemeter

the "outgassed" material to a gas chromatograph. This unit was a Model 311 manufactured by Carle Instruments, Inc. The detector column used was a 2.4 m column approximately 0.03 mm in diameter with a packing composed of 80 percent Pora Pak N and 20 percent Pora Pak Q. A flame ionization detector unit was used to identify the various hydrocarbon species after segregation by the column material. This type of detector essentially counts the number of carbon atoms in the various molecules and thus can identify the molecule as members of a tentative paraffinic series.

An infra-red absorption device was also used to analyze the soot composition, this was a Beckman IRA unit. In this method soot was mixed with hot carbon disulphide (CS_2) and the resulting solution was analyzed by examining the absorption spectra of a broad range infra-red beam passed through a sample of the solution.

In addition to the above, a scanning electron microscope (SEM) was used to examine the soot in detail for its morphological characteristics. The unit utilized was an AMR model 1210; this latter unit included energy dispersive spectroscopic analysis equipment which allowed individual particles to be analyzed. The spectroscopic mode used was the X-ray range and the method is

generally termed energy dispersive X-ray (EDX) analysis. The EDX analyzer was capable of detecting elements with atomic numbers between 12 and 48, and did so by examining the X-ray emission spectra after a particle had been "hit" with a focused high energy (25 KV) electron beam. Carbon with an atomic number of 6 thus could not be detected. Only a few elements exist besides carbon are solid at the analysis conditions with atomic numbers less than 12; boron, beryllium and lithium being the only examples. The chances of the particles being composed of any of the latter three elements is remote since none of those elements were part of or introduced into the test rig system. Thus the particles if they had no spectra could be identified as carbon.

3.4 TEST OPERATIONS

Before testing the primary zone equivalence ratio was set to a value of 0.5 by adjusting the primary and dilution port plugs. A constant pressure drop ($\Delta P/P$) of five percent, was maintained. The flow data necessary to set the plug positions was obtained by calibrating the combustor port openings on a special "cold flow" rig made available by Solar to the program.

The operation of the actual test apparatus involved light-off, design-point condition setting and shut-down. Light-off was accomplished by setting the inlet air flow a little below the desired value, and the air pressure to approximately 2.8 atm. A modified Solar engine torch igniter firing into the combustor primary zone was then supplied with air and fuel (JP-5) and ignited. The air pressure available to the torch which had a high pressure drop was limited to approximately 5.8 atm and this was the main reason that the combustor was lighted at low air pressures. With the torch burning fuel was then introduced into each of the combustor ports. When ignition of the combustor proper was indicated by the exhaust thermocouple, the fuel flow was adjusted to provide the desired outlet temperature. Following this, the air flow and pressure were increased in small steps interposed with fuel flow increases, until the desired levels were reached. Usually the outlet temperature during the light-off and the approach to the design point was maintained below 950°C. When the design point air pressure, temperature and mass flow was reached, the fuel flow was adjusted to the level necessary to provide the design point outlet temperature and the torch was shut-down. Shortly after this outlet temperature was set, water was introduced into the soot collection tube. Smoke sampling was also started. This procedure of maintaining the soot-tube hot until the design point conditions were reached ensured that any soot deposited was associated only with the design point.

If the design point outlet temperatures were below 950°C then the water was introduced directly after the conditions were reached. Once the design point conditions were reached (see Table 1 for a list of these operating points), the smoke meter was monitored for particulates. If no readings were obtained on the smoke meter, then the air inlet temperature was reduced, to reduce the vaporization premixed level, until smoke was indicated. In those instances, when no smoke was obtained with a reduction in inlet temperature to the minimum level (approximately 40°C), the pressure was reduced. Generally the temperature was increased to at least 150°C before the pressure was decreased and the procedure was repeated.

Table 1
Test Conditions

Test Point	Inlet Temperature (°C)	Inlet Pressure atm	Mass Flow kg/s	Fuel/Air Ratio	Premixing Proportion
Atmospheric Baseline	38 to 339	1	0.45	0.1-0.025	≈ 100% to ≈ 0%
Mid-Point Tests	38 to 339	4	0.45	0.01-0.025	≈ 100% to ≈ 0%
Medium Pressure Tests	38 to 339	10	0.45	0.01-0.025	≈ 100% to ≈ 0%
Part-Load	38 to 339	14	0.45	0.01-0.025	≈ 100% to ≈ 0%
Max-Load	38 to 339	16	0.45	0.01-0.025	≈ 100% to ≈ 0%

During shut-down operation the fuel was first diverted to a cell drum and air was allowed to blow-back through the fuel liners to a three-way solenoid that allowed the air and fuel to dump into a barrel type container. Then the fuel flow was stopped. By using this technique a sharp cut-off of the fuel flow was obtained and thus operation at a reduced fuel-air ratio was minimized as was the injection of raw fuel.

Immediately after the fuel flow was stopped the air flow was also shut down.

It was felt that the above technique provided a means of acquiring soot deposits at a specific set of conditions.

** no soot was obtained during the above procedure then the fuel-air or air-fuel ratio in the primary zone was increased by changing the position of the primary and dilution port plugs or valves. The pressure drop ($\Delta P/P$) was, however, maintained near constant between 4.5 percent and 5 percent.

4

RESULTS AND DISCUSSION

4.1 TEST OBJECTIVES

The major objective was to determine combustor operating conditions that would prevent the formation of soot. Specifically the desire was to find a level of premixing that would eliminate soot formation for any particular reaction or primary zone equivalence ratio.

The basis for pursuing this particular approach is provided below, through a consideration of the operating characteristics of conventional combustors.

In conventional combustion systems the combustion process is essentially heterogeneous and a wide range of local fuel/air ratios can exist. In such a process the fuel (usually an atomized liquid) and air are injected separately into the reaction zone of the combustor at a nominally stoichiometric fuel/air ratio (equivalence ratio of one). Because the mixing rate between fuel and air is finite and usually in gas turbines is less than the chemical oxidation rate the fuel/air ratio can locally be in excess of stoichiometric. In some combustors (FT-4 for example), see Reference 2, the combustion zone is sufficiently unmixed that it could be described as "stratified". Improved mixing as described in this latter reference (after the primary zone had been made lean to reduce high-power smoke associated with soot deposition) improved matters further and also reduced low-power unburned fuel "smoke" emissions.

The improvement in mixing in the case above was achieved by both the modification of the air jet distribution patterns and by improvements in atomization.

Smoke emission levels that meet all legislative requirements are in many cases sufficiently high to produce soot deposits on waste heat boilers. Unpublished work at Solar has revealed that a modified "no-smoke" combustor in a 3300 HP engine still produced soot deposits on a waste-heat boiler, even though no visible smoke emissions were normally present.

The general conclusion that can be derived from the above is that to avoid smoke or soot production all fuel rich areas in the reaction zone must be avoided completely. This automatically eliminates conventional heterogeneous combustion systems, because it would be necessary to prevaporize and premix the fuel and air prior to reaction, to avoid fuel-rich zones. Prevaporizing/premixing modifications to what generally would be thought of as a conventional combustor, have been devised by Mann-Turbomotoren and

others. Prior to this latter work, Solar had demonstrated a radically modified combustion system that utilized prevaporization and premixing of the fuel to obtain with a lean reaction zone ultra-low NO_x emissions and zero smoke levels. The history and data on this latter system is contained in References 3 and 4.

In general it is impractical to completely premix/prevaporize the fuel, and thus minimization of fuel rich areas can only be attained by reducing the overall fuel/air or equivalence ratio in the primary zone. This approach generally reduces peak fuel/air or equivalence ratios in addition to the mean values which effectively reduces the local level of "richness".

Thus two parameters can be identified as being important in the control of soot production; one being premixing and prevaporization which is probably the most critical and the other being the reduction in the reaction zone fuel/air or equivalence ratio. Both of these approaches appear to achieve a reduction in soot production by "attacking" the first step in the soot production scheme shown in Figure 14, that is the thermal decomposition step. Decreases in equivalence ratio may, however, also affect the "soot radical" production through increased oxidation which could provide aldehyde related radicals that block the reactions that produce polyacetylenes.

It should be noted that there will be, for any application, and particularly for gas turbine use, distinct limits imposed on both premixing and on the degree of equivalence ratio reduction. These limits are best illustrated by Figure 15 which indicates what is presently believed to be the general trends of the relationships between premixing and equivalence ratio reduction and soot formation. In practice a limit line parallel to the ordinate at some low value of the equivalence ratio can be superimposed on this graph to represent the lean extinction limit of the combustor reaction zone. This means that the value of this equivalence ratio will be that used with the lowest operating power point. By using the required turn down ratio (TDR) at maximum power point of the engine a second line at a higher equivalence ratio can be erected which delineates the complete engine operating range. In addition to these two lines a third curve (not known accurately) describing the fundamental autoignition limits for the fuel in question must also be considered. Such a curve is shown schematically in the above-mentioned figure. These three lines which abscina enclose an allowable operating area which defines in turn, the conditions over which testing will have to be conducted.

4.2 TEST RESULTS

The main point that can be made from the results of the testing performed is that it was very difficult to produce smoke or soot under partially premixed conditions.

Data showing the operating characteristics that produced soot are summarized in Table 2. It should be noted that many hours of "negative" testing were involved in obtaining these few results. The difficulties encountered in

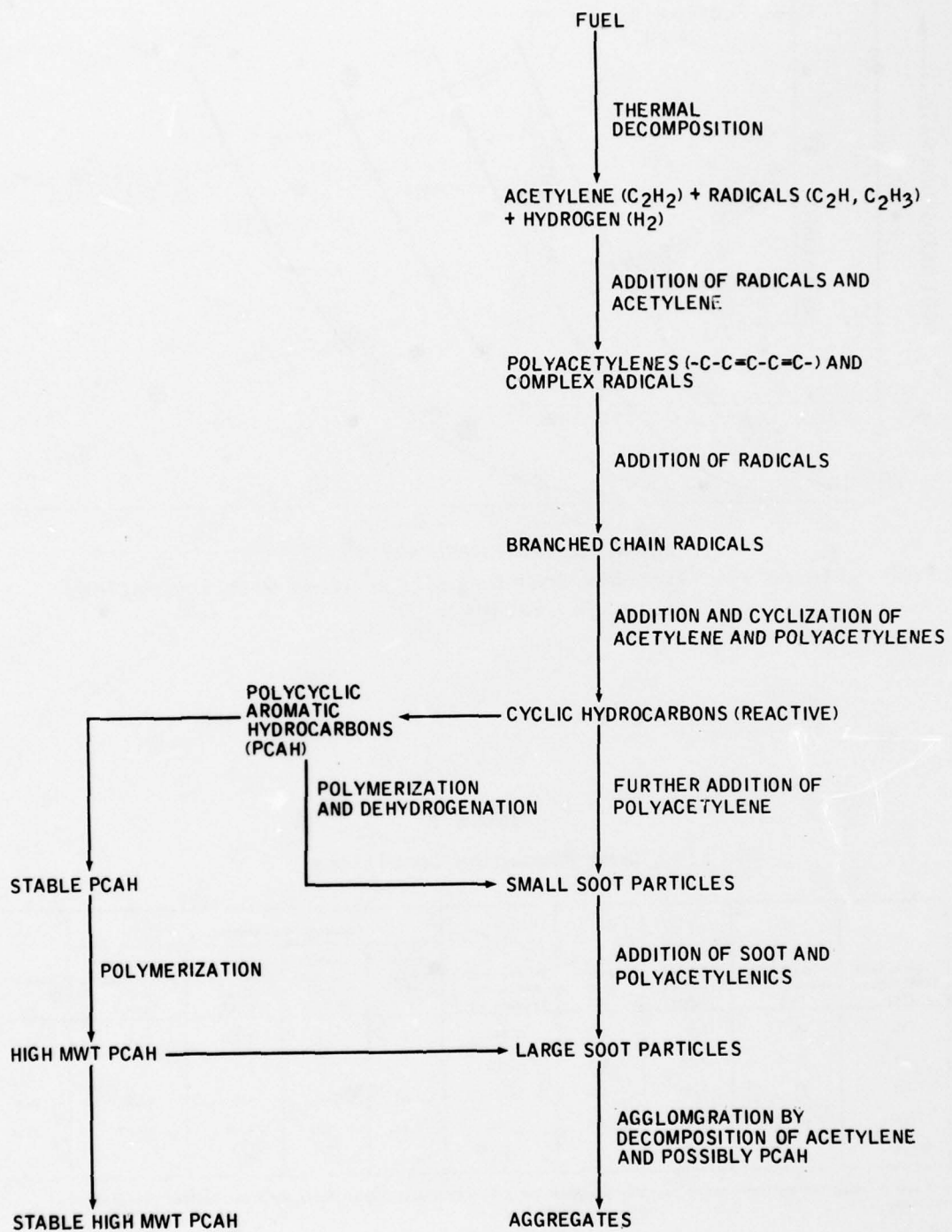


Figure 14. Possible Reaction Sequence for Soot Formation

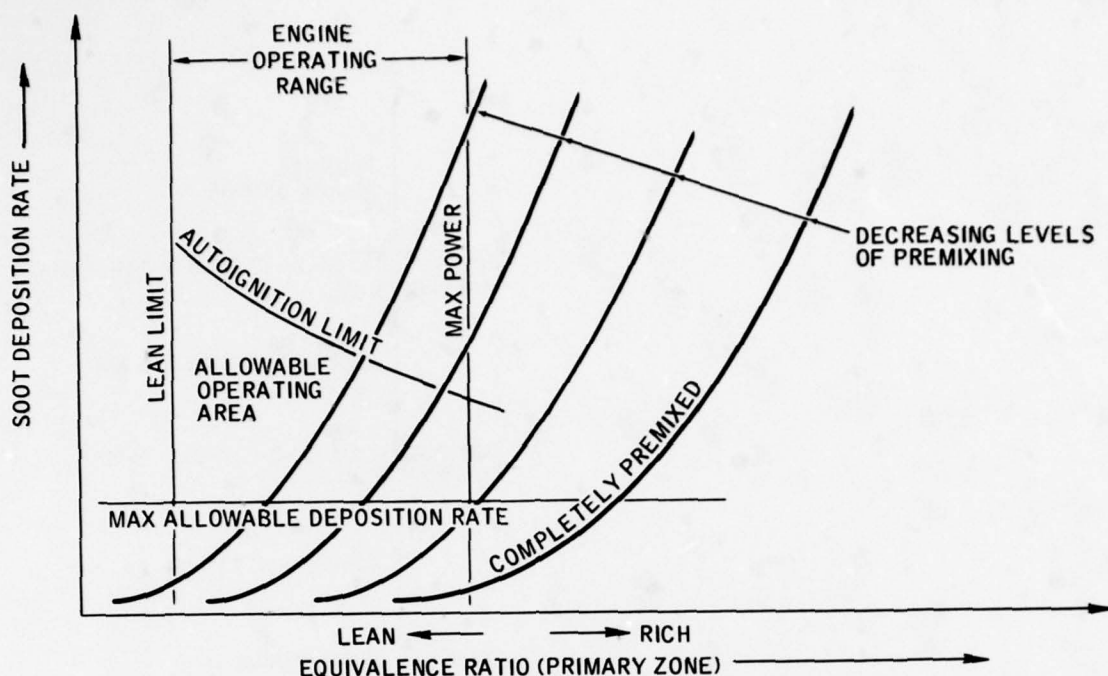


Figure 15. Probable Soot Deposition Rates With Combustion System Parameters

Table 2
Soot Producing Conditions

	Soot Tube Temperature (°C)	Inlet Air Temperature (°C)	Inlet Air Pressure (atm)	Pressure Drop ΔP/P (%)	Equivalence Ratio (φ) Primary Zone	Exhaust Emissions					Combustion Efficiency (%)
						Carbon Dioxide (CO ₂) (%)	Carbon Monoxide (CO) (g/Kg)	Oxides of Nitrogen (NO _x) (g/Kg)	Unburned Hydrocarbons (UHC) (g/kg)	Combustion Efficiency (%)	
1	78	32	2.0	3.3	0.836	5.1	37.7	2.69	22.0	96.9	
2	99	65.5	2.55	4.7	0.816	0	0	0	0	0	
3	93	77	2.69	4.7	1.06	3.07	61.4	2.2	31.3	95.4	
4	110	68	2.72	4.5	1.112	3.63	5.06	4.56	0.37	99.8	
5	110	38	3.0	4.1	1.473	0	0	0	0	0	

Note 4 and 5 exhibited positive smoke particle presence but negligible soot accumulation data points that provided soot deposition.

producing soot were not anticipated, and it took much longer than planned to obtain the data. At the conditions listed even though the combustor was operated in a "premixed" mode, the combustion must have taken place in a heterogeneous fashion. Little vaporization and thus little mixing could take place at the combustor operating conditions that produced the soot deposits.

Some observations can be made concerning the soot deposition. It was noticed that soot particles under fuel lean to stoichiometric conditions deposited and adhered better than soot particles produced under fuel rich conditions. Generally under lean to stoichiometric conditions the combustion efficiency had to be below 97 percent before soot was produced. In terms of exhaust emissions this meant that there would have to be carbon monoxide levels greater than 20 g/kg. Although under rich reaction conditions smoke was produced the particles did not appear to be capable of "sticking" to the probe surface.

For soot deposition at lean to stoichiometric reaction conditions, the onset of soot fouling on the probe correlated well with smoke detection. When the reaction or primary zone equivalence ratio is richer than stoichiometric the presence of smoke in the exhaust is not necessarily indicative of soot deposition.

The rate of soot deposition was low and varied between 2×10^{-5} g/s and 3×10^{-5} g/s depending on the primary zone equivalence ratio. The higher rates being associated with an equivalence ratio of 0.8 and the lower level with an equivalence ratio of 1.0.

The soot taken from the tube and the smoke particles collected on filter paper were both subjected to chemical analysis. The sample tube with a soot coating is shown in Figure 16. Carbon deposits were also found in the combustor during operation at sootting conditions and this is shown in Figures 17 and 18.

Pyrolysis chromatography was the basic method used to study soot samples taken from the tube. In all the cases tested, no hydrocarbons of any type were detected. To ensure that these results were not spurious a check was made by subjecting soot in carbon disulfide to an infra-red absorption analysis. As before, no positive identification of any hydrocarbons could be made. Essentially the spectra obtained (see Fig. 19) was that of carbon disulfide itself. An inorganic analysis was also made of the soot scraped from the surface of the tube. This showed that significant levels of iron (Fe), nickel (Ni) and chromium (Cr) and sulfur (S) were present together with several other trace elements (see Table 3). These latter metallic "impurities" were probably contaminants that were mixed with the soot during the tube scraping operations.

Energy Dispersive X-Ray (EDX) analyses of smoke particles trapped on filter paper however, showed no trace of the above metals or any element heavier than the limiting case of sodium. This latter analysis showed in effect that the particles had to be nearly pure carbon with possibly some hydrogen. When the EDX and the pyrolysis chromatography analyses are combined it is evident that the particles must have been pure carbon.

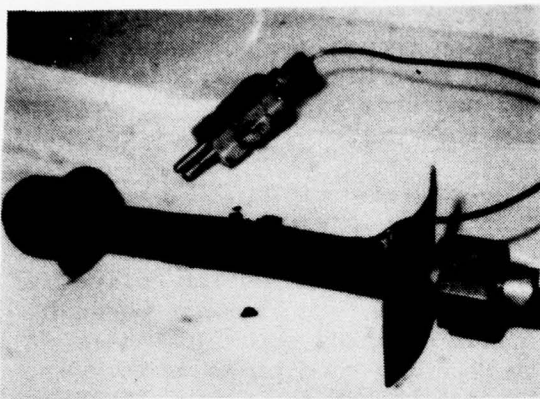


Figure 16.

Front View of Soot Collection Tube
With Soot Coating

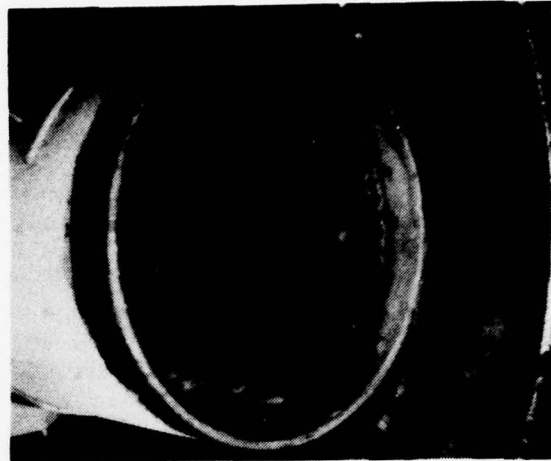


Figure 17.

Soot Deposits in Combustor Exhaust

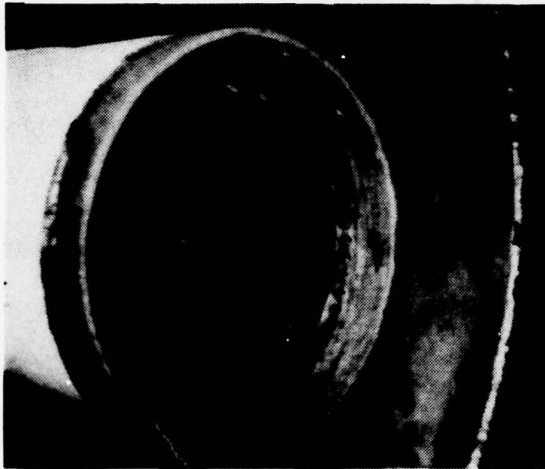


Figure 18.

Soot Deposits in Combustor Exhaust

Table 3
Inorganic Analysis

Elements Detected (Approx. %) - %			
Al 0.1	Fe 8.0	S 6.7	
C 66	K <0.1	Si 0.2	
Ca 0.2	Mo 0.3	Zn 0.2	
Cl 0.8	Ni 6.6		
Cr 1.1	P 0.1		
Cu 0.9	Pb 0.6		

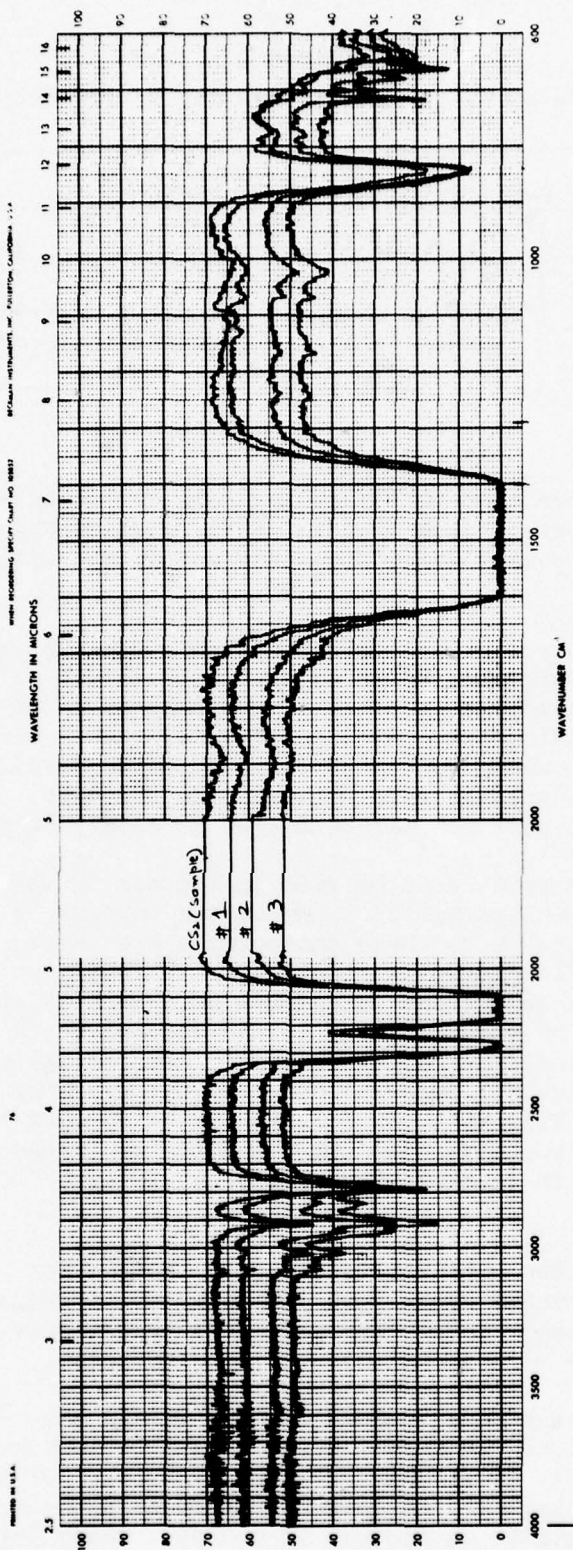


Figure 19. WFR-A-RED Absorption Spectra of Soot in CS₂

Table 4
Approximate Size Range for Various Deposition Mechanisms

Particle Diameter (D) Microns			
D<0.1	0.1<D<1.0	1<D<5	D<5
Molecular Diffusion	Brownian Motion (Randon walk)	Turbulent Diffusion	Inertial Impaction

Scanning Electron Microscopic (SEM) studies were conducted with the particles to determine their general morphology and also to allow EDX analyses to be made since the latter equipment required the use of the SEM chamber and "gun".

Several polaroid photographs were produced of the soot and smoke particles and in particular those smoke particles collected on filter paper were studied in detail. These latter figures were thought to be important because they showed typical agglomerate particle sizes and also possible "basic particle" sizes. A knowledge of these sizes provided details of the mechanism of how the particles were collected on the tube. Table 4 shows for example the probable deposition mechanism for a variety of particle sizes.

Typical particle agglomerates can be seen in Figures 20 and 21 which are filter paper samples with particles lying on the surface in addition to those that are buried. Particles on these photographs are white. Figure 20 is a 700X magnification while Figure 21 is a 1500X magnification and shows in detail the bottom left hand corner of Figure 20. Most of the large particles had the general shape of oblate spheroids and appeared to be made up of smaller roughly spherical particles. These latter particles although they varied in diameter somewhat, appeared to be in the range of 0.1 to 0.3 microns in diameter. This size was confirmed by a 12,000X magnification of a single filter paper fiber (Fig. 22) which had on its surface some small spherical particles. These particles ranged in size from 0.15 to 0.25 microns in diameter.

Other larger agglomerates appeared to be up of the smaller oblate spheroids to give a random structural appearance. Typical of these is a particle shown in Figure 23 which appears to be composed of several oblate spheroids, all of approximately the same size (0.042 mm) or (42 microns).

Two "close-up" pictures of the surface of this latter particle are shown in Figures 24 and 25. Figure 24 is a 12,000X magnification whereas Figure 25 is a 20,000X magnification. The basic botyoidal structure of the agglomerates is clearly shown in Figure 26. A further particle is shown in Figure 26 and two details of the particle in Figures 28 and 29. Basic particle sizes are shown clearly in these last figures.

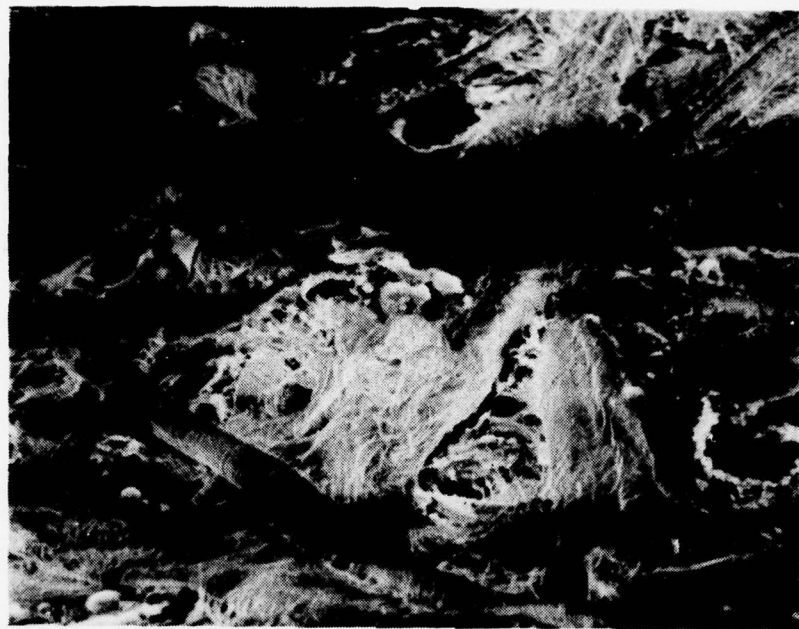


Figure 20. Smoke/Soot Particles on Filter Paper

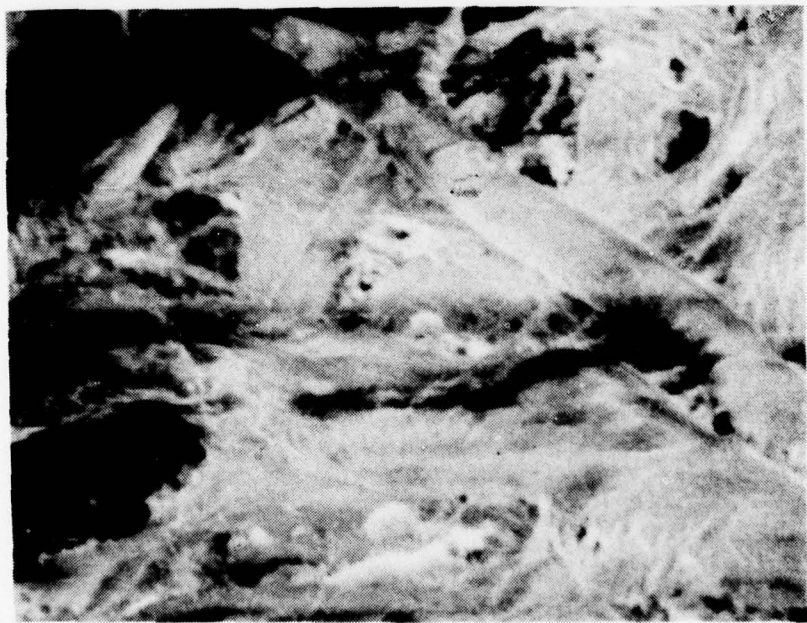


Figure 21. Smoke/Soot Particles on Filter Paper



**Figure 22. Single Fiber Showing Small Particles
(12,000X Magnification)**



**Figure 23. Compound Agglomerate Soot Particle
(600X Magnification)**



Figure 24. Detail of Smoke/Soot Particle

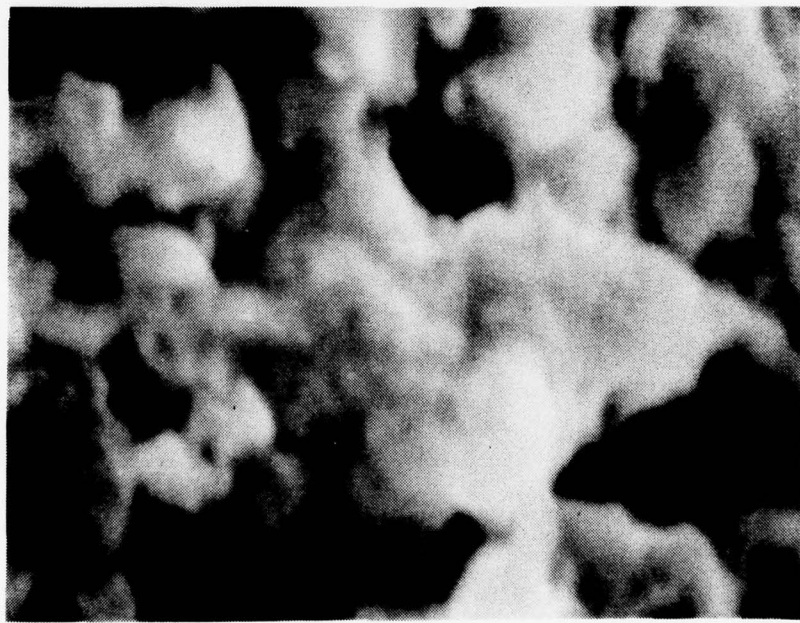


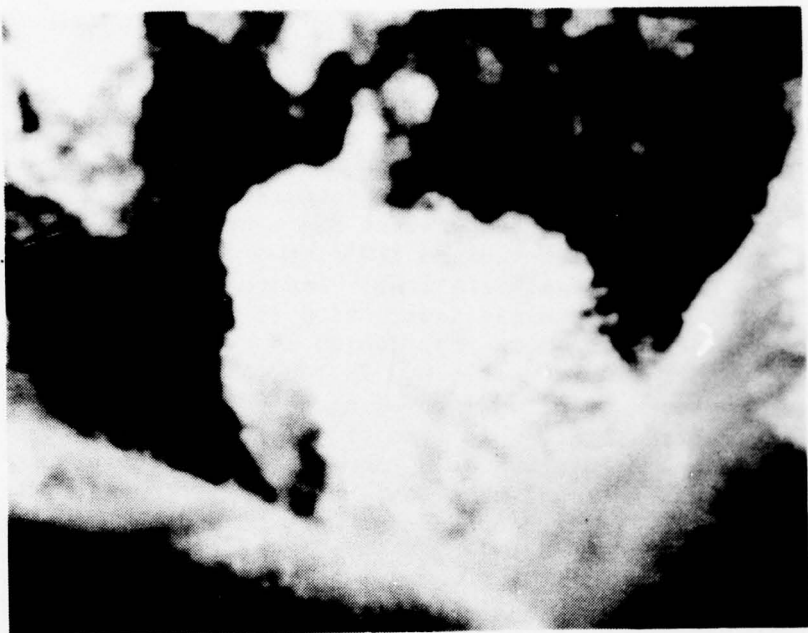
Figure 25. Detail of Smoke/Soot Particle Showing Typical Botryoidal Structure



Figure 26. Agglomerate Smoke Particle Showing Botryoidal Structure
(1800X Magnification)



Figure 27. Smoke/Soot Particle on Filter Paper
(600X Magnification)



**Figure 28. Detail of Particle of Figure 26
(12000X Magnification)**



**Figure 29. Detail of Particle of Figure 26
(18000X Magnification)**

4.3 DISCUSSION

From the analysis of the deposits on the tube it would appear that a layer of water was present on the tube surface. At the conditions that the system was operated at the exhaust should have a dewpoint of less than 38°C based on data of Reference 5. The tube temperature was considerably above this temperature, however, at a level circa 110°C, and thus no liquid water would be expected based on these considerations. Before testing the tube was pre-oxidized to avoid any possible interaction of the oxidation process with the soot. This oxidation process provides an adherent oxide film which protects the metal from further attack. In general this film is extremely adherent and is composed of mixed chrome, nickel and iron oxides probably with a spinel type structure. This type of material could adsorb water (ceratin chrome spinel oxides are used commercially for this purpose), however, no data could be found to allow the use of Freundlich, Langmiur or Brunauer Emmett and Teller's theories (see Refs. 6 and 7), to calculate the likely concentrations. Carbon which the air borne particles were composed of also adsorbs water and thus if such a particle impacted the tube surface, it could possibly adhere through adsorption forces with water as the intermediate "glue".

Adsorption occurs on the surface of the solid tube wall coating and generally results from valence forces or other attractive forces of the atoms or molecules in the outermost layer of the solid coating. Adsorption covers usually two types of sorption physical adsorption and chemisorption. The forces causing physical adsorption are similar to those that cause the condensation of a gas to form a liquid. Any heat evolved upon physical adsorption is small and such adsorption is completely reversible. In chemisorption the heat evolved is much larger and it may be considered that a surface compound is formed. It is thought however that physical adsorption would be the main mechanism by which the carbon particles could adhere to the surface. Generally for a given adsorbent (given surface area) the amount of material adsorbed depends on the concentration or partial pressure of the material around the adsorbent. Thus after the first layer of carbon is deposited more water could be adsorbed onto the new surface (which is now larger) and if more carbon particles impacted the sample tube they could adhere by the same adsorption forces.

4.4 DEPOSITION

From an analysis of the carbon particle sizes found, four basic mechanisms of deposition have been identified as possible modes, these are (1) molecular diffusion, (2) Brownian motion (random walk), (3) turbulent diffusion, and (4) inertial impaction. Each of these mechanisms is applicable to a particular range of particle sizes, although the absolute values of the ranges involved is not well known. In addition there are probably particle sizes in which two mechanisms of are of roughly equal importance.

Particles with diameters below 0.1 micron behave like large molecules and molecular diffusion controls the deposition of such sized material. Maxwell's Law of Diffusion describes the chemical diffusion mechanism where there is a partial pressure gradient in the direction of diffusion.

If two materials are considered one (A) which is adsorbed on a surface and the other (B) which is not, then a partial pressure gradient will be set up causing A to diffuse towards, and B away from the surface, see Figure 30.

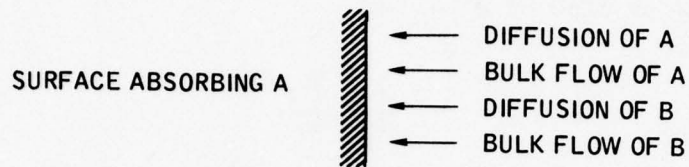


Figure 30. Diffusion Scheme for an Adsorbing Surface

It can be shown that the rates of diffusion of A and B are given by

$$N_A = -D \cdot \frac{\partial C_A}{\partial y} = -\frac{D}{RT} \cdot \frac{\partial P_A}{\partial y} \quad (1)$$

and $N_B = +D \cdot \frac{\partial C_B}{\partial y} = +\frac{D}{RT} \cdot \frac{\partial P_B}{\partial y} \quad (2)$

For equimolecular counterdiffusion where the total pressure (P) is constant throughout the system $P = P_A + P_B$

thus $P = P_A + P_B = RT(C_A + C_B) = RT \left(\frac{C_A}{M_A} + \frac{C_B}{M_B} \right) \quad (3)$

so that $\frac{\partial P_A}{\partial y} = -\frac{\partial P_B}{\partial y}$

$$\frac{\partial C_A}{\partial y} = -\frac{\partial C_B}{\partial y}$$

and $\frac{\partial C_A}{\partial y} = - \frac{\partial C_B}{\partial y} \cdot \frac{M_A}{M_B}$

A will be absorbed at the surface and B will tend to diffuse away and therefore a total pressure gradient will be produced causing a bulk motion of A and B towards the surface, in addition to the transfer by diffusion. Since there is no net motion of B, the bulk rate of flow must exactly balance its transfer by diffusion.

Thus the bulk rate of flow of B = $-N_B$

$$= \frac{D}{RT} \frac{\partial P_A}{\partial y}$$

The bulk flow of B is accompanied by a bulk flow of A, equal to

$$N_B \cdot \frac{P_A}{P_B} = - \frac{D}{RT} \cdot \frac{P_A}{P - P_A} \cdot \frac{\partial P_A}{\partial y} \quad (\text{from equations 1, 2, and 3}) \quad (4)$$

This bulk rate of flow produces a velocity u_F , given by

$$u_F \cdot \frac{P_A}{RT} = - \frac{D}{RT} \cdot \frac{D}{P - P_A} \cdot \frac{\partial P_A}{\partial y}$$

$$u_F = - \frac{D}{P - P_A} \cdot \left(\frac{\partial P_A}{\partial y} \right) \quad (5)$$

The total rate of transfer of A, N'_A , is obtained by adding the rates given in equations (1) and (4)

$$N'_A = - \frac{D}{RT} \cdot \left(1 + \frac{P_A}{P - P_A} \right) \cdot \frac{\partial P_A}{\partial y}$$

$$= - \frac{D}{RT} \cdot \frac{P}{P - P_A} \cdot \frac{\partial P_A}{\partial y} \quad (6)$$

This relation is known as Stefan's Law (Ref. 8).

Integration of the above equation between two positions denoted by suffixes 1 and 2, gives

$$N_A' = \frac{D \cdot P}{RT(y_2 - y_1)} \ln \left(\frac{P - P_{A2}}{P - P_{A1}} \right) \quad (7)$$

$$= \frac{D \cdot P}{RT(y_2 - y_1)} \ln \left(\frac{P_{B2}}{P_{B1}} \right)$$

$$= \frac{D \cdot P}{RT(y_2 - y_1)P_{Bm}} (P_{B2} - P_{B1})$$

(where P_{Bm} is the logarithmic mean of P_{B1} and P_{B2})

$$= - \frac{D \cdot P}{RT(y_2 - y_1)P_{Bm}} \cdot (P_{A2} - P_{A1}) \quad (8)$$

$$= - \frac{D \cdot C_T}{(y_2 - y_1)C_{Bm}} \cdot (C_{A2} - C_{A1}) \quad (9)$$

where C_T and C_{Bm} are the total molar concentration and the logarithmic value of C_B respectively.

Equation (7) can be simplified if P_A is small compared with P , giving

$$\begin{aligned} N_A' &= \frac{D \cdot P}{RT(y_2 - y_1)} \ln \left(1 - \frac{P_{A2} - P_{A1}}{P - P_{A1}} \right) \\ &= \frac{D \cdot P}{RT(y_2 - y_1)} \cdot \left(- \frac{P_{A2} - P_{A1}}{P - P_{A1}} - \dots \right) \\ &\approx - \frac{D}{RT(y_2 - y_1)} \cdot (P_{A2} - P_{A1}) \end{aligned} \quad (10)$$

To apply this type of relationship to soot deposition requires the assumption that all the gas species can be "lumped together" and treated as a single material, (B). Whereas the soot would be treated as A. Similarly water vapor could be assigned to A and everything else in the system to B. Only order of magnitude rates can be obtained however from the above equations, because of a lack of knowledge of the partial pressures or concentrations of carbon, the diffusivity, and the distances ($y_2 - y_1$) over which the gradient exists. For carbon particles of the order of 0.05 to 0.1 microns in diameter it is estimated that the deposition rate in $\text{g/cm}^2/\text{s}$ is the same order as the concentration in g/cm^3 .

It is worthwhile pointing out at this time that molecular mass transfer is controlled by the identical flow parameters which control convective heat transfer. Relationships have been derived which relate mass transfer to convective heat transfer (Ref. 9, 10, 11). McAdams (Ref. 12) indicates how the terms in the convective heat-transfer equations may be revised so as to convert the equations to a mass-transfer relationship. The observations can be made that, if there are small particles in a gas stream, then the deposit rate increases as the convective heat-transfer coefficient increases and decreases as the fraction of heat transfer by radiation is increased with a constant total heat-transfer rate. Thus waste heat boilers should be ideal small particle collectors.

When the particles are of the order of 0.1 to 1.0 microns in diameter. Brownian effects tend to dominate the particle motion and thus the deposition rate. Generally under these latter conditions, minimal deposition rates are obtained although it is difficult to assign any specific values to the rates. Most of the measured smaller "basic" particle sizes fell into this range, which might explain the difficulties encountered in producing adherent soot layers.

The discussion of Brownian motion involves two important points: (1) the part that Brownian motion plays in the deposition of particles which are larger than 0.1 micron and still too small to be hurled through the boundary layer by turbulent motion, and (2) the role of Brownian motion in the deposition of particles less than 0.1 micron in diameter.

The upper limit to Brownian-motion considerations is not clear cut. It is usually assumed that some sort of random-walk technique controls deposition so long as the particles are too small to be hurled through the boundary layer by stream turbulences. However, at some size, the particles begin to "see" not only a continuum but the whirles and eddies in it. They become unable to follow these turns, however, and are thrown into quieter regions, such as boundary layers. The mechanism proposed is that particles are on the average hurled a distance of one stopping distance into the laminar boundary layer (where the stopping distance is the distance required for the particle to lose all of its momentum). The travel of the particles the remaining distance to the wall is then controlled by Brownian motion.

If particles are large enough (over 1 micron in diameter) to be hurled through the boundary layer (in other words, if the stopping distance is greater than the boundary-layer thickness), then the deposition rate becomes a function of friction factor and essentially independent of particle size.

Whenever the stopping distance is a factor in deposition, the surface roughness becomes important. This is because the stopping distance increases with increases in the initial velocity of the particle. The initial velocity results from turbulence which in turn is a function of surface roughness. A new boiler, for example, is reported to stay clean for a relatively long period of time. However, once deposits start, they build up at a rapid rate. This form of deposition is often referred to as turbulent diffusion controlled.

Inertial impaction occurs when the particles are too large (of the order of 10 microns and larger) to follow all of the turns and velocity changes which the stream encounters in approaching an obstacle. For example, as the gas accelerates and decelerates around a tube, a particle could, if large enough, continue to move towards the tube and collide with it. A review of the extensive literature on inertial impaction can be found in the work of Golovin and Putnam (Ref. 13).

When only inertial forces are considered then for cylindrical collectors such as boiler tubes, various analyses (see Ref. 14, 15, 16 and 17) can be utilized to produce the curves shown in Figure 31 which correlate efficiency of impaction or deposition versus an inertial correlation parameter (Ψ).

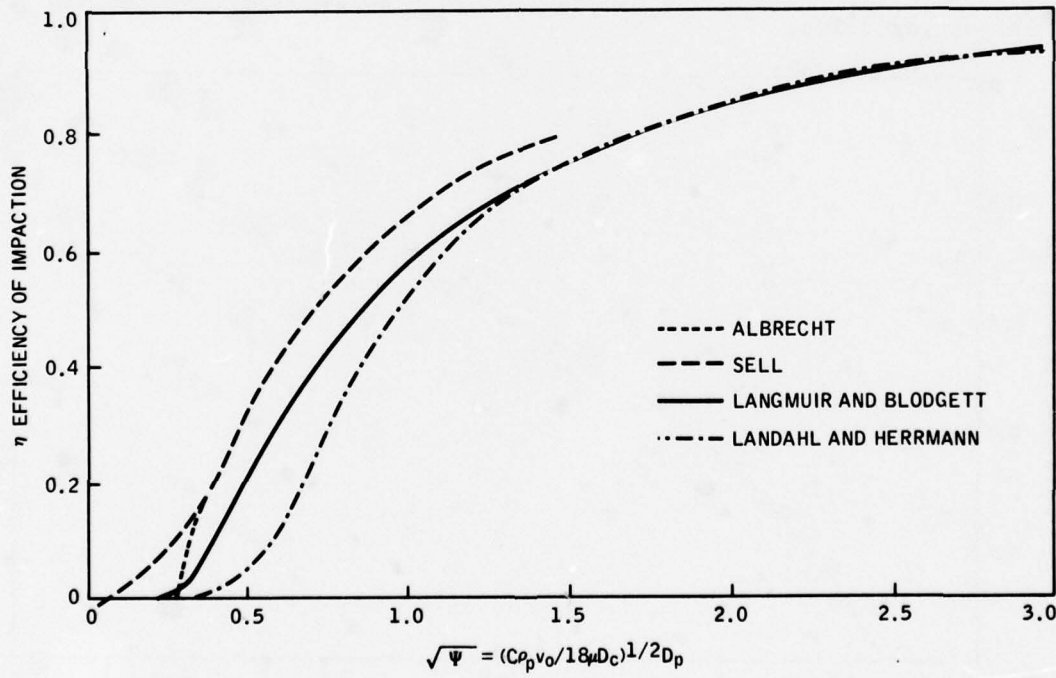


Figure 31. Theoretical Inertial Collection Efficiencies for a Cylindrical Body

$$\text{where } \Psi = C \rho_p v_o D_p^2 / 18 \mu D_c$$

and C = empirical constant
 ρ_p = particle density
 D_p = particle diameter
 D_c = collector diameter
 μ = fluid viscosity

Ψ is the ratio of the force necessary to stop a particle initially traveling at a velocity v_o in the distance $D_p/2$, to the fluid resistance at a relative particle velocity of v_o . It is also the ratio of the stopping distance - i.e., the distance a particle will penetrate into still air when given an initial velocity of v_o - to the diameter of the collector.

The above results have been generally verified by the experimental work of Ranz and Wong (Ref. 18) who determined the curve shown in Figure 32. As can be seen the curve follows the same trends as Figure 31, however, no efficiencies greater than 0.8 were obtained.

The experimental apparatus used was designed so that the impaction efficiency parameter (Ψ)^{1/2} was in excess of 2.5, thus ensuring a constant collection efficiency. This ensured the highest possible collection efficiencies for the larger particles.

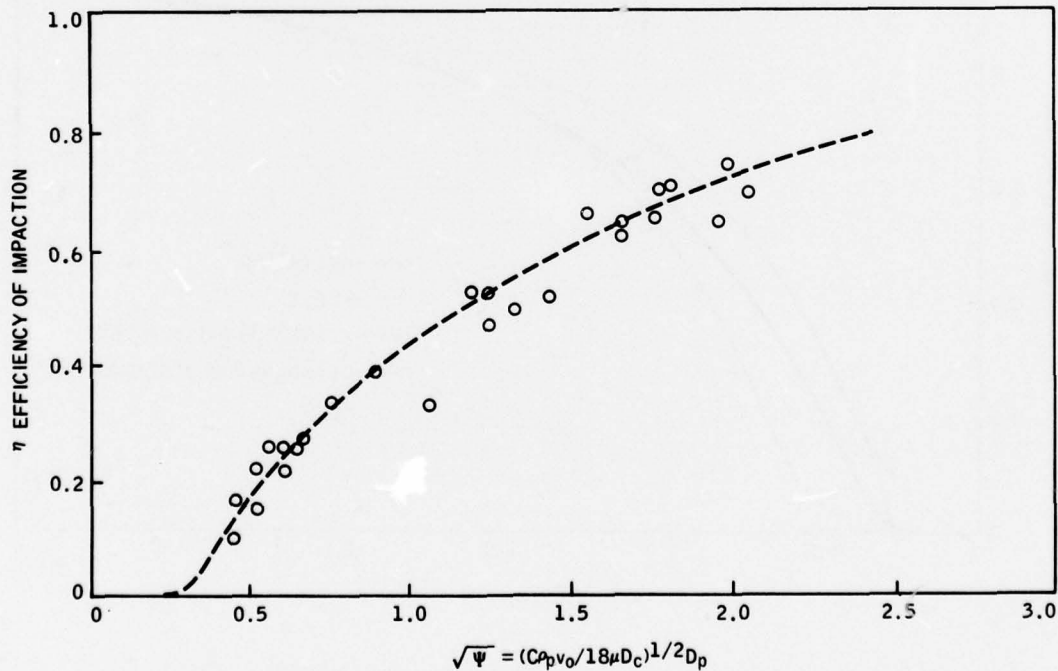


Figure 32. Experimental Intertial Collection Efficiencies for a Cylindrical Body

A summary of the above discussion is provided by Figure 33 which shows the deposition rates found with a 2.5 cm diameter tube. Each of the deposition mechanisms and its associated particle size range has been identified.

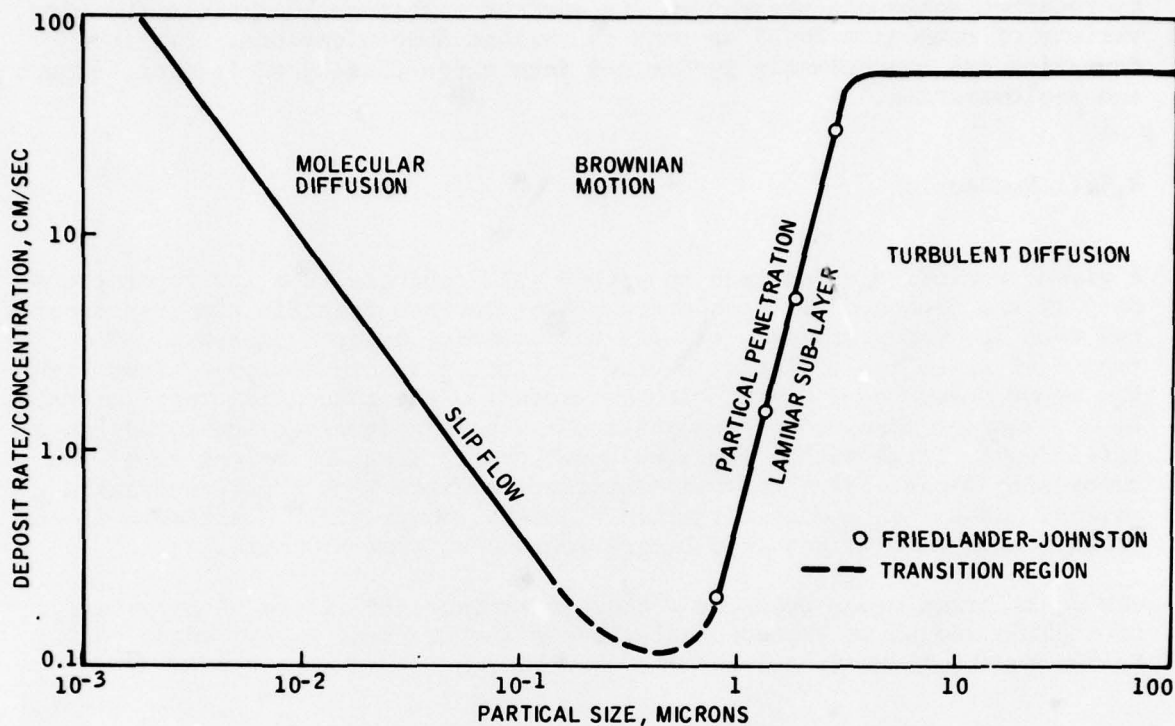


Figure 33. Deposition Rate on a 2.5 cm Tube

4.5 PARTICLE FORMATION

Experimental work on the formation of soot from gaseous hydrocarbons is plentiful but often apparently contradictory and difficult to understand. The mechanisms advocated (see, for example Gaydon & Wolfhard 1970; Homann 1967) include dehydrogenation and polymerization via acetylenes, polymerization via aromatics, condensation and graphitization, nucleation on unspecified uncharged species and nucleation on ions, but none of these mechanisms has been put on a firm quantitative footing.

Evidence for the various mechanisms has largely been gleaned from analyses of the various compounds associated with the carbon in soot deposits. In past work (see Refs. 1 and 19) polycyclic aromatic hydrocarbons (PCAH) and polyacetylenes were identified in soot deposits and this presence was used to justify a theory of polymerization via polyacetylenes. More recent work at Solar (Ref. 20) has shown that when hydrocarbons are present they are often

paraffinic compounds and few if any aromatic species are found. One possible explanation for this is proposed by Jensen (Ref. 21) in which a particle formation method is proposed that includes homogeneous nucleation from carbon vapor and subsequent growth of a carbon nucleus. The carbon particle so formed could, if it passed through a fuel-rich zone, adsorb the various hydrocarbon compounds present on its surface. This could explain the wide variety of compounds found in soot by various investigations. Particle formation can conveniently be divided into three phases, nucleation, growth and agglomeration.

4.5.1 Nucleation

A given chemical species such as carbon will condense from the vapor phase only in the presence of a condensed phase (certain specific chemical species) and when its vapor pressure exceeds the saturation vapor pressure. The second of these two criteria is often satisfied in combustion systems with the vapor pressure of C_2 for example exceeding the saturation vapor pressure by an order of magnitude. Homogeneous nucleation involves the formation of sufficiently large nuclei for subsequent growth from the molecules of the condensing vapor. Usually such formation requires high super saturation ratios. Classical theory on particle growth can provide an estimate of the nucleus size that is required before subsequent growth occurs.

The equilibrium vapor pressure P above a surface (of radius of curvature r) of a condensed phase exceeds that above a flat surface P_0 according to the Kelvin equation, when:

$$\ln (P/P_0) = 2\eta v/rkT, \quad (11)$$

where η is the surface free energy, v the molecular volume in the condensed phase, k the Boltzmann constant and T the temperature. Consequently, for a given super-saturation ratio S condensation may occur on a spherical droplet of radius r when

$$r \leq r_c = 2\eta v/kT \ln S. \quad (12)$$

Smaller droplets (with higher vapor pressures) "evaporate" and do not, therefore, contribute to homogeneous nucleation. Droplets with $r < r_c$ may grow indefinitely.

It is difficult to calculate r_c for carbon, not least because of the large uncertainties concerning η and S in combustion and pyrolysis systems. It is unlikely that η is as high as $2 \times 10^{-4} \text{ J cm}^{-2}$ or S as low as 100 under conditions where soot formation is about to occur, however, and r_c as given by equation (12) is therefore unlikely to be as large as 0.3 nm ($\text{v} \sim 10^{-23} \text{ ml}$). A carbon fragment of this size contains only a few atoms, and it is clearly unreasonable to assign to it a bulk condensed phase value for η . The

calculation does suggest that a species containing only a few atoms of carbon may be responsible for the homogeneous nucleation of carbon vapor. Significantly, there is nothing in the classical calculation to suggest that species as small as C_2 and C_3 are not capable of inducing homogeneous nucleation.

The formation of small soot particles from such nuclei may be treated, to a first approximation as irreversible.

There are many chemical reaction schemes that can be proposed to produce potential nuclei such as C_2 , even from single carbon atom molecules such as methane (CH_4). A typical reaction set for methane is shown in Table 5. This table also includes reactions for ethane and ethylene (reaction 4 and 6, which are often produced as cracking fragments). Rice and Herzfeld (Ref. 22) developed a free-radical chain mechanism to explain the general features of paraffinic hydrocarbon decomposition. This was later modified by Rice and Kossiukoff (R-K) (Ref. 22) to include isomerization by ring formation. The results of this analysis agree well with experimental data on the decomposition of n-hexadecane and isododecane, (Ref. 24), both these compounds, it should be noted, are constituents of the fuel used. This decomposition model shows that most of the material ends up as ethylene, ethane and propylene. This fits into the above reaction scheme well.

4.5.2 Growth

Candidates for the initial nucleus on which coagulation and growth may begin are C_2 , C_3 and C_2H . It is reasonable to suggest (cf. Tesner, Snegiriova and Knorre (Ref. 25) C_2 , C_3 , C_2H and C_2H_2 as "growth species" - i.e. molecules which are assimilated into a particle, physically or chemically, upon collision of the molecule with the particle surface. A series of particle growth terms analogous to those for chemical reaction may then be written; e.g., for the irreversible conversion



$$-d[C_i]/dt = d[C_{i+1}]/dt = k_{2i}[C_i][C_2H_2]$$

$$\text{and } -d[C_2H_2]/dt = d[H_2]/dt = k_{1i}[C_i][C_2H_2],$$

with $(n_{i+1} - n_i)k_{2i} = 2k_{1i}$ for C_2 , C_2H and C_2H_2 growth species. Values of k_{1i} are listed in Table 6; they are based on the assumption that each collision of a growth species at a particle surface results in assimilation of the growth species into the particle. Collision rates have been calculated from simple kinetic theory. The neglect of diffusion terms does not introduce significant kinetic theory. The neglect of diffusion terms does

Table 5
Gas-Phase Reaction Mechanism and Rate Coefficients

reaction	rate coefficient	equilibrium constant	uncertainty factor
1 $\text{CH}_3 + \text{H} \rightarrow \text{CH}_4$	1.7×10^{-13}	$1.7 \times 10^{-38} \exp(51300/T)$	30
2 $\text{CH}_4 + \text{H} \rightarrow \text{CH}_3 + \text{H}_2$	$3 \times 10^{-10} \exp(-6000/T)$	$24 \exp(-30/T)$	10
3 $\text{CH}_3 + \text{CH}_2 \rightarrow \text{C}_2\text{H}_5$	$1 \times 10^{-10} \exp(-1400/T)$	$2.1 \times 10^{-37} \exp(43600/T)$	10
4 $\text{C}_2\text{H}_5 + \text{H} \rightarrow \text{C}_2\text{H}_6 + \text{H}_2$	$2 \times 10^{-10} \exp(-6000/T)$	$9.4 \exp(1360/T)$	3
5 $\text{C}_2\text{H}_6 + \text{H} \rightarrow \text{C}_2\text{H}_5 + \text{H}_2$	$2.8 \times 10^{-10} \exp(-20400/T)$	$9.3 \times 10^{32} \exp(-17000/T)$	5
6 $\text{C}_2\text{H}_5 + \text{H} \rightarrow \text{C}_2\text{H}_6 + \text{H}_2$	$3 \times 10^{-11} \exp(-3460/T)$	$6.3 \exp(-550/T)$	10
7 $\text{C}_2\text{H}_6 + \text{M} \rightarrow \text{C}_2\text{H}_5 + \text{H} + \text{M}$	$3.6 \times 10^{-7} \exp(-16600/T)$	$3.6 \times 10^{34} \exp(-20400/T)$	30
8 $\text{C}_2\text{H}_5 + \text{H} \rightarrow \text{C}_2\text{H}_4 + \text{H}_2$	$3 \times 10^{-10} \exp(-9500/T)$	$4.6 \exp(-2600/T)$	100
9 $\text{C}_2\text{H}_4 + \text{H} \rightarrow \text{C}_2 + \text{H}_2$	$1 \times 10^{-10} \exp(-18000/T)$	$2.3 \exp(-16000/T)$	30
10 $\text{N}_i + \text{G} \rightarrow \text{C}_a (+ \frac{1}{2} \text{pH}_2)$	1×10^{-10}	—	—

N_i , initial nucleus; G , growth species; ν is integral; $N_i \equiv C_3$ or $C_2\text{H}$; $G \equiv C_2$, C_2H or C_2H_2 .

Origins of rate coefficients are given in the appendix.

Units of rate coefficients: one molecule reactions, $\text{ml molecule}^{-1} \text{s}^{-1}$; two molecule reactions, $\text{ml}^2 \text{molecule}^{-2} \text{s}^{-1}$; three molecule reactions, $\text{ml}^3 \text{molecule}^{-3} \text{s}^{-1}$.

Uncertainty factors ω are such that k_u and k/l provide rough upper and lower bounds respectively to rate coefficients k .

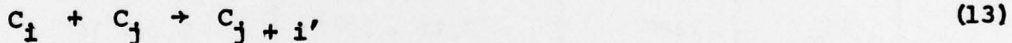
not introduce significant error into the application described below, but under other experimental conditions it may be necessary to include such terms.

Although only C_2 , C_2H and C_3 are regarded as initial nuclei and C_2 , C_2H , C_3 and C_2H_2 as growth species in an explicit sense, the growth treatment implicitly allows molecules containing four or more carbon atoms (e.g., the intermediates observed by Bonne, Homann & Wagner (Ref. 26) to participate, in so far as contributions from these species are accounted for by the averaged conversion terms for C_A , C_B , When reliable kinetic and thermochemical data for such molecules become available, it will be possible to make explicit allowance for their reactions, with consequent gains in physical insight into the early stages of particle formation.

4.5.3 Agglomeration

In order to calculate agglomeration rates the continuum distribution of soot particle radii is replaced by a discrete distribution with specified particle size ranges and averaged rates of conversion from one size range to another. The radii of 15 particles for the application described below are given in Table 6. Although soot may contain small proportions of elements of other than carbon, it is convenient to treat the particles as if they were pure carbon in the interests of preserving a simplified mass balance.

All particles except the largest were permitted to agglomerate irreversibly with all others via inclusion of rate terms for processes of the type



where $r_{Ci} > r_{Cj}$ and i runs alphabetically from A to O. For these processes,

$$-\frac{d[C_i]}{dt} = k_{\alpha ij} [C_i] [C_j] \quad (14)$$

$$\text{and} \quad -\frac{d[C_j]}{dt} = \frac{d[C_{j+i}]}{dt} = k_{\beta ij} [C_i] [C_j], \quad (15)$$

where $(n_{j+1} - n_j) k_{\beta ij} = n_i k_{\alpha ij}$ and the i th particle contains n_i carbon atoms. For $i \equiv j$, conversion terms of the type

$$-\frac{d[C_i]}{dt} = 2k_{\alpha ii} [C_i]^2, \quad \frac{d[C_{i+1}]}{dt} = 2k_{\beta ii} [C_i]^2, \quad (16)$$

Table 6
Particle Radii and Growth Rate Terms

Species	Radius/nm	Carbon Atoms Per Particle, n_i	$K_{li}/\text{ml Molecule}^{-18^{-1}}$
C_A	0.2	4	1.4×10^{-10}
C_B	0.38	23	6.0×10^{-10}
C_C	0.95	360	3.2×10^{-9}
C_D	2.3	5080	1.9×10^{-8}
C_E	5.7	7.8×10^4	1.2×10^{-7}
C_F	15	1.44×10^6	8.2×10^{-7}
C_G	32	1.32×10^7	3.6×10^{-6}
C_H	63	1.06×10^8	1.4×10^{-5}
C_I	150	1.47×10^9	8.3×10^{-5}
C_J	380	2.32×10^{10}	5.2×10^{-4}
C_K	790	2.07×10^{11}	2.2×10^{-3}
C_L	1600	1.66×10^{12}	9.0×10^{-3}
C_M	3800	2.31×10^{13}	5.2×10^{-2}
C_M	7900	2.07×10^{14}	2.2×10^{-1}
C_O	16000	1.66×10^{15}	--

with $n_i + 1 K_{\beta ii} = n_i K_{\alpha ii}$, were included. Values of K_{α} are given in Table 7. They are based on two main assumptions: (1) that the unit concentration collision rate v for two particles of radius r_1 and r_2 respectively is given by

$$v = (NkT\bar{v}/2)^{1/2} \{ (r_1^3 + r_2^3) (r_1 + r_2)^4 r_1^{-3} r_2^{-3} \}^{1/2} \quad (17)$$

where \bar{v} is the specific (atomic carbon) condensed phase volume of 1×10^{-23} ml and N the Avogadro number; and (2) that the sticking probability for two

Table 7
Coagulation Rate Terms

Values tabulated are those of κ and κ' (ml particle $^{-1}$ s $^{-1}$) as defined in the text, at 1600 K. For $C_A + C_B \rightarrow C_K$, for example, $-\frac{d[C_K]}{dt} = 2.7 \times 10^{-6} [C_A][C_B]$ particle ml $^{-1}$ s $^{-1}$ and $-\frac{d[C_J]}{dt} = \frac{d[C_K]}{dt} = 2.7 \times 10^{-6} \kappa' (C_A - C_J) [C_K]$ particle ml $^{-1}$ s $^{-1}$. $A(-B) \equiv A \times 10^{-3}$.

C_4	C_5	C_6	C_7	C_8	C_9	C_{10}	C_{11}	C_{12}	C_{13}	C_{14}	C_{15}	C_{16}	C_{17}	C_{18}	C_{19}	C_{20}
$6.3(-10)$	$1.0(-9)$	$3.7(-9)$	$1.8(-8)$	$6.5(-8)$	$2.8(-7)$	$1.1(-6)$	$6.5(-5)$	$4.1(-4)$	$1.8(-3)$	$7.0(-3)$	$4.1(-2)$	$1.8(-1)$	$-$	$-$	$-$	$-$
$-$	$8.7(-10)$	$2.0(-9)$	$7.7(-9)$	$4.0(-8)$	$2.6(-7)$	$1.1(-6)$	$4.3(-6)$	$2.5(-5)$	$1.0(-4)$	$6.7(-4)$	$2.7(-3)$	$1.6(-2)$	$6.7(-2)$	$-$	$-$	$-$
$-$	$-$	$1.4(-9)$	$3.0(-9)$	$1.2(-8)$	$7.0(-8)$	$2.9(-7)$	$1.1(-6)$	$6.3(-6)$	$3.9(-5)$	$1.7(-4)$	$6.8(-4)$	$3.9(-3)$	$1.7(-2)$	$-$	$-$	$-$
$2.1(-9)$	$4.7(-9)$	$8.1(-9)$	$2.2(-8)$	$8.2(-8)$	$3.1(-7)$	$1.7(-6)$	$1.1(-5)$	$4.5(-5)$	$1.8(-4)$	$1.0(-3)$	$4.5(-3)$	$-$	$-$	$-$	$-$	$-$
$-$	$-$	$3.4(-9)$	$6.6(-9)$	$8.1(-9)$	$2.5(-8)$	$8.7(-8)$	$4.6(-7)$	$2.7(-6)$	$1.2(-5)$	$4.6(-5)$	$2.7(-4)$	$1.2(-3)$	$-$	$-$	$-$	$-$
$-$	$-$	$-$	$-$	$-$	$9.8(-9)$	$2.6(-8)$	$1.2(-7)$	$6.7(-7)$	$2.8(-6)$	$1.1(-5)$	$6.2(-5)$	$2.7(-4)$	$-$	$-$	$-$	$-$
$-$	$-$	$-$	$-$	$-$	$7.9(-9)$	$1.3(-8)$	$4.8(-8)$	$2.4(-7)$	$0.5(-7)$	$3.7(-6)$	$2.1(-5)$	$8.9(-5)$	$-$	$-$	$-$	$-$
$-$	$-$	$-$	$-$	$-$	$1.1(-8)$	$2.4(-8)$	$9.8(-8)$	$3.6(-7)$	$1.3(-6)$	$7.5(-6)$	$3.2(-5)$	$-$	$-$	$-$	$-$	$-$
$-$	$-$	$-$	$-$	$-$	$1.7(-8)$	$-$	$3.9(-8)$	$1.2(-7)$	$4.0(-7)$	$2.1(-6)$	$8.7(-6)$	$-$	$-$	$-$	$-$	$-$
$-$	$-$	$-$	$-$	$-$	$-$	$-$	$2.8(-8)$	$-$	$4.9(-8)$	$1.3(-7)$	$5.9(-7)$	$2.3(-6)$	$-$	$-$	$-$	$-$
$-$	$-$	$-$	$-$	$-$	$-$	$-$	$-$	$4.0(-8)$	$6.7(-8)$	$2.4(-7)$	$8.5(-7)$	$-$	$-$	$-$	$-$	$-$
$-$	$-$	$-$	$-$	$-$	$-$	$-$	$-$	$-$	$5.6(-8)$	$1.2(-7)$	$3.6(-7)$	$-$	$-$	$-$	$-$	$-$
$-$	$-$	$-$	$-$	$-$	$-$	$-$	$-$	$-$	$-$	$6.7(-8)$	$1.5(-7)$	$-$	$-$	$-$	$-$	$-$

colliding particles is unity. This gives K_a and K_g values for the larger particles which are considerably bigger than would be consistent with the Smoluchowski theory (Ref. 27; see also Ref. 28). In general, the agglomeration rates of the larger particles do not play major roles in determining the overall soot conversion rate. Under conditions where this is not the case, proper allowance for the fact that equation (17) gives the correct collision rates only for $r < \lambda$ (the mean free path) must be made.

The results obtained indicated that there were few basic particles greater than 0.3 microns in diameter (150 nm in radius). This would suggest that at this size the agglomeration rate exceeded the growth rate. This latter condition is possible both the the scheme proposed above. Thus most particles with dimensions greater than 0.3 microns would be agglomerates with a general botryoidal appearance, and this is what has been found.

4.6 GENERAL

It should be noted that during the experimental evaluation it was found that it was extremely difficult to produce soot even at typical conventional combustor primary zone equivalence ratios (1.0 to 1.1). This difficulty is attributed to the premixing (at least partially of the fuel and air) which minimized the production of fuel rich zones or areas in the primary or reaction zone. By minimizing the size and number of fuel rich zones the local carbon particle pressure is reduced and potential of nucleation and condensation is minimized. By minimizing nucleation the first step in particle formation, the total soot level is minimized.

5

CONCLUSIONS AND RECOMMENDATIONS

The simplest and most significant conclusion is that it is difficult to produce soot or smoke when the fuel-air charge to the combustor is partially premixed. This is true even at equivalence ratios typical of conventional primary or reaction zones. It has been difficult to assess accurately the degree of vaporization and mixing required to avoid soot, however, using unpublished Solar work the vaporization level was estimated to be of the order of 12 percent. Rather than vaporization being the main factor, there may be some critical droplet size which when reached effectively, eliminates the possibility of fuel-rich decomposition reactions. This latter hypothesis is provided with some support by recent work performed at Solar and which will be published by the Electric Power Research Institute.

A hypothesis has been postulated regarding the formation, collection, and adhesion of soot to boiler tubes. This hypothesis explains the results of the present program while allowing for past work in the same field. If the hypothesis is correct, then if a coating or material which did not adsorb water is chosen for the boiler tubes no soot should adhere.

In addition if the fuel and air can be mixed sufficiently prior to reaction such that the carbon vapor in any fuel pocket cannot become super-saturated, then no soot or smoke should be produced.

It is recommended that further work be performed to verify the simple approach of partially premixing the fuel and air charge to eliminate soot formation. In addition any investigation of coatings or materials of construction for boiler tubes should include a consideration of those materials that do not adsorb water. Typically such materials would include certain glasses and ceramics.

Further work to verify the premixing of fuel and air effects on soot formation or rather the elimination of soot formation, should be performed on conventional combustion systems as a developmental effort. Typically "add-on" fuel-air premixing devices could be designed and incorporated into existing conventional combustors and then evaluated as to their effectiveness in soot prevention.

REFERENCES

1. D'Alessio, A., et al., "Soot Formation in Methane-Oxygen Flames", Fifteenth Symposium on Combustion, p. 1427.
2. Koblisch, T. R. and Schwartz, H. R., "Reduction of Low Power Smoke Emissions From an Industrial Gas Turbine Engine."
3. White, D. J., Roberts, P. B. and Compton, W. A., "Low NO_x Emission Combustor for Automobile Gas Turbine Engines", Final Report for EPA Contract 68-04-0016 (APTD-1441) prepared by Solar Turbines International an International Harvester Group (Feb. 1973).
4. White, D. J., Roberts, P. B., and Compton, W. A., "Solar JIC-B Combustor Development for Baseline Gas Turbine Engine", Final Report for ERDA contract 68-01-0464, prepared by Solar Turbines International, an International Harvester Group (March 1976).
5. Verhoff, F. H. and Banchero, J. T., "Predicting Dew Points of Flue Gases", Chemical Engineering Progress, Vol. 70, No. 8, August 1974.
6. Langmuir, J. Am. Chem. Soc. 38, 2267 (1916); 40, 1361 (1918).
7. Brunauer, Emmett and Teller, J. Am. Chem. Soc., 60, 309 (1938).
8. Stefan, J., Wiener Akad. Wissenschaft. 68 (1873) 385; 79 (1879) 169; 98 (1889) 1418; Ann. Physik 41 (1890) 723. Versuche über die Verdampfung.
9. Ungar, E. W., and Putnam, A. A., "An Analysis of the Deposition of Small Particles from a Moving Gas Stream by the Diffusion Process", AF 49(600)-710, January 1958.
10. Spalding, D. B., "Some Fundamentals of Combustion", Academic Press, Inc., New York 1955.
11. Punte, C. L., "Some Aspects of Particle Size in Aerosol Studies", Armed Forces Chemical Journal, 12, 28 (1958).
12. McAdams, W. H., "Heat Transmission", 3rd Edition, McGraw-Hill, New York, 1954.
13. Golovin, M. N., and Putnam, A. A., "The Intertial Impaction of Small Particles", AF 49(600)-710, January 1958.
14. Albrecht, F., Physik, Z., 32, 48 (1931).

15. Landahl, H. D., and Herrmann, R. G., J. Colloid Sci., 4, 103, 1949.
16. Langmuir, I., and Blogett, K. B., General Electric Research Laboratory, Schenectady, NY, Rept. RD-225, 1944-45.
17. Sell, W., Forsch. Gebiete Ingenieurw., 2, Forschungsheft., 347.
18. Ranz, W. E. and Wong, J. B., Technical Report No. 4, SO-1005, Technical Information Service, United States Atomic Energy Commission, Oak Ridge, TN.
19. Tompkins and long, Twelfth Symposium on Combustion, p. 625.
20. Roberts, P. B. and Kubasco, A. J., "Combined Steam Generator Gas Side Fouling Evaluation", Dept. of Navy SR79-R-4537-20, Contract No. N0024-77-C-4366 (to be published).
21. Jensen, D. E., "Prediction of Soot Formation Rates: A New Approach", Proc. R. Soc. Lond. A.338, 375-396 (1974).
22. Rice, F. O. and Herzfeld, K. F., J. Am. Chem. Soc, 56, 284 (1934).
23. Rice, F. O. and Kossiakoff, J. Am. Chem. Soc, 65, 590 (1943).
24. Voge, H. H. and Good, G. M., J. Am. Chem. Soc, 71, 593 (1949).

DISTRIBUTION LIST

	<u>No. of Copies</u>
Office of Naval Research 800 N. Quincy Street Arlington, VA 22217 Attn: Power Program, M. Keith Ellingsworth Technology Group	3 1
Defense Documentation Center Bldg. 5 Cameron Station Alexandria, VA 22314	12
Naval Research Laboratory 4555 Overlook Avenue Washington, DC 20390 Attn: Technical Information Division	12
U.S. Naval Post Graduate School Monterey, CA 93940 Attn: Dept. of Mechanical Engineering Dept. of Aeronautics	1 1
U.S. Naval Academy Annapolis, MD 21402 Attn: Dept. of Mechanical Engineering Dept. of Aeronautics	1 1
Office of Naval Research Branch Office 1030 East Green Street Pasadena, CA 91106 Attn: Mr. B. J. Cagle	1
Naval Air Systems Command Jefferson Plaza Washington, DC 20360 Attn: Propulsion Administrator, Code 330	1
Naval Sea Systems Command Crystal Plaza Washington, DC 20360 Attn: Ship Main Propulsion & Energy Br., Code 0331	1

Naval Ship Engineering Center
National Center
Washington, DC 20360
Attn: Propulsion Systems, Code 6140B 1

Naval Ship R&D Center
Annapolis, MD 21402
Attn: Power Systems Division
Gas Turbine Branch 1 1

Army Research Office
P.O. Box 12211
Research Triangle Park, NC 27709
Attn: Mr. James J. Murray 1

Air Force Office of Scientific Research
Bolling Air Force Base
Washington, DC 20332
Attn: Directorate of Aerospace Sciences 1

National Science Foundation
1800 G Street NW
Washington, DC 20550
Attn: Div. of Engineering, Heat Transfer Program 1

Department of Energy
Washington, DC 20545
Attn: Div. of Power Systems, Components & Heat Engines Branch 1

University of Arizona
Aerospace & Mechanical Engineering Dept.
College of Engineering
Tucson, AZ 85721
Attn: Professor Don McEligot 1

Naval Weapons Center
China Lake, CA 93555
Attn: Code 3161, Dr. W. Theilbar 1

University of Minnesota
Department of Mechanical Engineering
Minneapolis, MN 55455
Attn: Professor E. R. G. Eckert 1

Energy Research and Generation
Lowell & 57th Streets
Oakland, CA 94608
Attn: Dr. Glendon M. Benson 1

UNCLASSIFIED

SECURITY CLASSIFICATION OF THIS PAGE (When Data Entered)

REPORT DOCUMENTATION PAGE		READ INSTRUCTIONS BEFORE COMPLETING FORM
1. REPORT NUMBER SR79-R-4643-03	2. GOVT ACCESSION NO.	3. RECIPIENT'S CATALOG NUMBER
4. TITLE (and Subtitle) EFFECTS OF GAS TURBINE COMBUSTION ON SOOT DEPOSITION		5. TYPE OF REPORT & PERIOD COVERED Final - 10/15/77-3/79
7. AUTHOR(s) D. J. WHITE		6. PERFORMING ORG. REPORT NUMBER 6-4643-7
8. PERFORMING ORGANIZATION NAME AND ADDRESS Solar Turbines International 2200 Pacific Highway San Diego, CA 92138		9. CONTRACT OR GRANT NUMBER(s) N00014-78-C-0003
11. CONTROLLING OFFICE NAME AND ADDRESS (Code 613A:MAC) Procuring Contracting Officer - ONR Dept. of the Navy - 800 Quincy Street Arlington, VA 22217		10. PROGRAM ELEMENT, PROJECT, TASK AREA & WORK UNIT NUMBERS Unknown
14. MONITORING AGENCY NAME & ADDRESS (if different from Controlling Office) Defense Contract Admin. Service Management Area San Diego, Bldg. 4 AF Plant 19, 4297 Pacific Highway, San Diego, California 92110		12. REPORT DATE March 1979
		13. NUMBER OF PAGES 58 (including table of contents and cover page)
		15. SECURITY CLASS. (of this report) Unclassified
		16a. DECLASSIFICATION/DOWNGRADING SCHEDULE Unclassified
16. DISTRIBUTION STATEMENT (of this Report) <i>Approved for public release; Distribution Unlimited</i>		
17. DISTRIBUTION STATEMENT (of the abstract entered in Block 20, if different from Report) <i>Approved for public release; Distribution Unlimited</i>		
18. SUPPLEMENTARY NOTES		
19. KEY WORDS (Continue on reverse side if necessary and identify by block number) Soot, Combustion, Gas Turbine Heat Exchanger, Boiler, Heat Recovery		
20. ABSTRACT (Continue on reverse side if necessary and identify by block number) The effects of premixing the reaction air and fuel of a gas turbine combustor on soot formation were investigated. Other parameters such as pressure, temperature and reaction zone fuel-air ratio were also evaluated. Soot formation was found to be dominated by fuel-air premixing and could be suppressed readily through a partial premix process.		

